ปฏิกิริยาการขจัดน้ำของเอทานอลบนตัวเร่งปฏิกิริยาวัสดุเชิงประกอบอะลูมินาซิลิกา

นางสาวฐิตินันท์ จันทร์เชย

วิทยานิพนธ์นี้เป็นส่วนหนึ่งของการศึกษาตามหลักสูตรปริญญาวิศวกรรมศาสตรมหาบัณฑิต
สาขาวิชาวิศวกรรมเคมี ภาควิชาวิศวกรรมเคมี
คณะวิศวกรรมศาสตร์ จุฬาลงกรณ์มหาวิทยาลัย
ปีการศึกษา 2556

THE ETHANOL DEHYDRATION OVER AL-SI COMPOSITE CATALYSTS

Miss Titinan Chanchuey

A Thesis Submitted in Partial Fulfillment of the Requirements
for the Degree of Master of Engineering Program in Chemical Engineering
Department of Chemical Engineering
Faculty of Engineering
Chulalongkorn University
Academic Year 2013

Thesis Title	THE ETHANOL DEHYDRATION OVER AL-SI COMPOSITE CATALYSTS
By	Miss Titinan Chanchuey
Field of Study	Chemical Engineering
Thesis Advisor	Associate Professor Bunjerd Jongsomjit, Ph.D.

Accepted by the Faculty of Engineering, Chulalongkorn University in Partial Fulfillment of the Requirements for the Master's Degree

.....Dean of the Faculty of Engineering

(Professor Bundhit Eua-arporn, Ph.D.)

THESIS COMMITTEE

.....Chairman

(Associate Professor Muenduen Phisalaphong, Ph.D.)

.....Thesis Advisor

(Associate Professor Bunjerd Jongsomjit, Ph.D.)

.....Examiner

(Assistant Professor Suphot Phatanasri, D.Eng.)

.....External Examiner

(Ekrachan Chaichana, D.Eng.)

ฐิตินันท์ จันทร์เชย : ปฏิกิริยาการขจัดน้ำของเอทานอลบนตัวเร่งปฏิกิริยาวัสดุเชิงประกอบอะลูมินาซิลิกา. (THE ETHANOL DEHYDRATION OVER AL-SI COMPOSITE CATALYSTS) อ.ที่ปรึกษาวิทยานิพนธ์หลัก: รศ. ดร. บรรเจิด จงสมจิตร, 80 หน้า.

ในงานวิจัยนี้ศึกษาคุณลักษณะและความว่องไวของตัวเร่งปฏิกิริยาวัสดุเชิงประกอบอะลูมินาซิลิกา และตัวเร่งปฏิกิริยาโมลิบดินัมบนอะลูมินาซิลิกา ตัวเร่งปฏิกิริยาวัสดุเชิงประกอบอะลูมินาซิลิกามีการเปลี่ยนแปลงจำนวนของอะลูมินาในช่วงระหว่างร้อยละ 20 ถึง ร้อยละ 80 โดยน้ำหนัก หลังจากนั้นอัตราส่วนที่ดีที่สุดของตัวเร่งปฏิกิริยาวัสดุเชิงประกอบอะลูมินาซิลิกาคือการให้ความว่องไวของการเกิดปฏิกิริยาดีที่สุด ถูกทำให้เต็มไปด้วยจำนวนของโมลิบดินัมในช่วงระหว่างร้อยละ 1 ถึง ร้อยละ16 โดยน้ำหนัก ความว่องไวของทุกตัวเร่งปฏิกิริยาจะถูกแสดงผ่านการเปลี่ยนแปลงของเอทานอล และการเลือกเกิดของผลิตภัณฑ์ในปฏิกิริยาการขจัดน้ำของเอทานอล คุณลักษณะของทุกตัวเร่งปฏิกิริยาถูกอธิบายลักษณะโดยใช้การดูดซับทางกายภาพด้วยไนโตรเจน การกระเจิงรังสีเอกซ์ การส่องผ่านด้วยกล้องจุลทรรศน์อิเล็กตรอน การกระจายตัวของโลหะ การดีซอฟชันของแอมโนเนียแบบโปรแกรมอุณหภูมิ และการส่องกราดด้วยกล้องจุลทรรศน์อิเล็กตรอน การเพิ่มขึ้นของอะลูมินาส่งผลต่อลักษณะทางสัณฐานวิทยา และความเป็นกรด ลักษณะทางสัณฐานวิทยาถูกเปลี่ยนแปลงจากอนุภาคทรงกลมกลายเป็นกลุ่มของอนุภาค ในส่วนของความเป็นกรด กรดอ่อนจะมีจำนวนน้อยที่สุด แต่กรดปายกลางถึงกรดแก่มีจำนวนมากที่สุดที่ร้อยละ 60 โดยน้ำหนักของอะลูมินาบนซิลิกา หรือ 60Al-SSP นอกจากนี้ตัวเร่งปฏิกิริยาวัสดุเชิงประกอบ 60Al-SSP ให้ค่าสูงที่สุดทั้งในค่าของการเปลี่ยนแปลงเอทานอลและการเลือกเกิดเป็นเอทิลีน ในการทำให้ 60Al-SSP ให้เต็มไปด้วยจำนวนของโมลิบดินัมที่มากขึ้นมีอิทธิพลกับการกระจายตัวของโมลิบดินัมและความเป็นกรด สำหรับความเป็นกรดนั้น กรดอ่อนถูกทำให้เพิ่มมากขึ้น ในทางตรงกันข้าม กรดปานกลางถึงกรดแก่ถูกทำให้ลดลงหลังจากเติมโมลิบดินัมด้วยจำนวนที่มากขึ้น เมื่อพิจารณาที่ความว่องไว พบว่าลำดับของการเลือกเกิดเอทิลีนสอดคล้องกับผลของกรดปานกลางถึงกรดแก่ การเปลี่ยนแปลงเอทานอลของร้อยละ 1 โดยน้ำหนักของโมลิบดินัมบน 60Al-SSP ให้ค่าสูงที่สุด ขณะที่จำนวนของโมลิบดินัมมากกว่าร้อยละ 5 โดยน้ำหนักบน 60Al-SSP แสดงค่าความว่องไวต่ำกว่าของตัวเร่งปฏิกิริยาวัสดุเชิงประกอบ 60Al-SSP

ภาควิชา วิศวกรรมเคมี ลายมือชื่อนิสิต .....

สาขาวิชา วิศวกรรมเคมี ลายมือชื่อ อ.ที่ปรึกษาวิทยานิพนธ์หลัก .....

ปีการศึกษา 2556

5570175521 : MAJOR CHEMICAL ENGINEERING
KEYWORDS: ETHANOL DEHYDRATION

TITINAN CHANCHUEY: THE ETHANOL DEHYDRATION OVER AL-SI COMPOSITE CATALYSTS. ADVISOR: ASSOC. PROF. BUNJERD JONGSOMJIT, Ph.D., 80 pp.

This research investigated the characteristics and catalytic activity of Al2O3-SiO2 composite catalyst and molybdenum supported Al2O3-SiO2. The Al2O3-SiO2 composite catalyst which was various amount of alumina ranged from 20wt% to 80wt%. After that the best ratio of Al2O3-SiO2 composite catalyst which exhibited the highest catalytic activity was impregnated by amount of molybdenum ranged from 1wt% to 16wt%. The catalytic activity of all catalysts was represented through ethanol conversion and selectivity of products in ethanol dehydration reaction. The characteristics of all catalysts were characterized by BET surface area, XRD, SEM, EDX, NH3-TPD and TEM methods. The increasing of alumina affected the morphology and acidity. The morphology was changed from spherical particle to cluster. In part of acidity, the weak acid site was minimum, but the medium-strong acid site had maximum at 60wt% of alumina on silica (60Al-SSP). Moreover, the 60Al-SSP composite catalyst gave the highest both ethanol conversion and ethylene selectivity. Impregnation of 60Al-SSP with higher amount of molybdenum had influence with distribution of molybdenum and acidity. For the acidity, the weak acid site was increased, whereas the medium-strong acid site was decreased after adding more molybdenum. Considering the catalytic activity, it was found that the order of ethylene selectivity agreed with result of medium-strong acid site. The ethanol conversion of 1wt% of molybdenum on 60Al-SSP was the highest while the amount of molybdenum more than 5wt% on 60Al-SSP exhibited lower activity of 60Al-SSP composite catalyst

Department:	Chemical Engineering	Student's Signature	.....
Field of Study:	Chemical Engineering	Advisor's Signature	.....
Academic Year:	2013		

ACKNOWLEDGEMENTS

The author would like to evince her appreciation and gratefulness to her advisor, Assoc. Prof. Dr. Bunjerd Jongsomjit for his guidance, counsel, guidelines for solving problem and supervision along this study. Furthermore, she is thankful to Assoc. Prof. Dr. Muenduen Phisalaphong, as a chairman, Asst. Prof. Dr. Suphot Phatanasri and Dr. Eakrachan Chaichana as the members of the thesis committee.

Thankful for assistance and graceful suggestion to Mr. Jakrapan Janlamool, Dr. Mingkwan Wannaborworn and each friends in the laboratory who always provision the furtherance and co-worker thorough this study.

Finally, the author would like to state her gratitude to her parents for encouragement, support and carefulness.

CONTENTS

Page

Page

Page

LIST OF TABLES

Page

LIST OF FIGURE

Page

CHAPTER I

INTRODUCTION

1.1 General introduction

Ethylene is classified as the light olefins. It has been commonly used in various chemical industries, such as manufacture polyethylene, vinyl chloride (from ethylene dichloride), and styrene (from ethyl benzene) [1]. Those mentioned chemicals are considered to be important raw materials for production wares in our daily life. Therefore, as the number of population has been increasing, the extensive global demand of large capacity of ethylene results in the high cost of ethylene.

Nowadays, the reduction and insufficient amount of fossil fuel, which is the major source of ethylene production, is still the main problem in petrochemical industry. Ethylene has been produced by hydrocarbon steam cracking process [1] which can generate numerous types of product [1]. However, some products from that process can cause the environmental problem. In addition, the purification process of ethylene is required leading to high investment and operating cost. Therefore, the new beneficial methods of ethylene production process need to be established.

The ethanol dehydration is novel promising way of ethylene production. The ethylene from this process is environmental friendly because using ethanol as raw material can reduce to utilization of fossil fuel. Moreover, ethanol can be generated by common fermentation process from renewable and agriculture products, such as bagasse, corn, and cassava. Those raw materials for ethanol production are the products commonly found in Thailand [1]. Therefore, this process can not only reduce the cost and the usage of fossil fuel, but also provide higher capacity of ethylene. This leads to the increasing trend of number of articles studies on ethanol dehydration in 1998-2012 [1, 2].

In chemical reactions, the catalysts are an important factor because it helps to accelerate and control the rate of reaction. The catalysts have many types and have

been used in different chemical reactions. The ethanol dehydration to ethylene requires acid catalysts because active site of this reaction has to desire acidity. The acid catalysts in industry system have many types, such as modified-Al_2O_3, Al-Si Oxide, Al_2O_3-MgO/SiO_2, ZSM-5, HZSM-5 [2, 3], SAPO-34, and heteropolyacid catalysts [2]. In previous studies, the modified-Al_2O_3 catalysts were used in high temperature to generate high selectivity of ethylene product. However, the HZSM-5 catalyst and the heteropolyacid ($Ag_3PW_{12}O_{40}$) were not stable. They can cause the coke formation due to high acidity [1]. The Al-Si oxide catalysts which are unmodified catalyst, are barely used in ethanol dehydration, but used in other reaction. The rational advantages of using alumina and silica catalysts are that the SiO_2 is suitable to be a support due to the high surface area, excellent mechanical strength, uniform pore size and thermal stability, especially hexagonal mesoporous silica in M41S family such as MCM-41 and spherical silica particle (SSP) [3]. Al_2O_3 is a good support due to its high metal dispersion ability and excellent mechanical properties [4].

The performance of catalyst is possibly increased by adding some metal oxide on the support or elementary catalyst such as Re_2O_7/Al_2O_3, WO_3/SiO_2, MoO_3/Al_2O_3 in olefin metathesis reaction [5], Co_3O_4/Al_2O_3-SiO_2 in cyclohexane nitrosation to **ε**-caprolactam [6] etc. For the ethanol dehydration reaction to ethylene, it reacts on acid site of catalyst. So, the metal oxide gives higher acidity in catalyst, then be interesting. The molybdenum oxide is the metal oxide, that helping increase amount of acidity in the catalyst. The industries system, the molybdenum oxide over oxide supports was used in various reactions which required acid site for active site such as MoO_3/Al_2O_3-SiO_2 in light olefin metathesis or partial oxidation [7, 8] MoO_3/ZrO_2 in hydrolysis of ethyl acetate and MoO_3/Al_2O_3 in hydrodesulfurization of thiophene [9] etc. However, the molybdenum oxide is hardly used in ethanol dehydration reaction, then it should be investigated.

1.2 Research objectives

To investigate characteristics and the effect of different Al loading on the spherical silica particle (SSP). Al-SSP composite supported molybdenum catalysts on the activity and selectivity during ethanol dehydration to ethylene.

1.3 Research scopes

- Preparation of spherical silica particle (SSP).
- Characterization of silica support samples by BET surface area, X-ray diffraction (XDR), scanning electron microscopy (SEM), and temperature programmed desorption (TPD).
- Preparation of Al_2O_3-SiO_2 (Al-SSP) composites catalyst with 20 to 80 %wt. of Al_2O_3 on SSP support using hydrolysis of aluminium isopropoxide method.
- Characterization of Al_2O_3-SiO_2 (Al-SSP) composites catalysts by BET surface area, X-ray diffraction (XDR), scanning electron microscope (SEM) and energy x-ray spectroscopy (EDX) and temperature programmed desorption (TPD).
- Investigation of the catalytic activity of Al_2O_3-SiO_2 (Al-SSP) catalysts in ethanol dehydration at 1 atm and 200-400^{o}C.
- Preparation of supported molybdenum oxide on the Al_2O_3-SiO_2 (Al-SSP) composite catalysts, which provide high selectivity of ethylene, using the incipient wetness impregnation method.
- Characterization of molybdenum oxide/Al_2O_3-SiO_2 (Mo_rO_q/Al-SSP) composites catalysts by BET surface area, X-ray diffraction (XDR), scanning electron microscope (SEM) and energy x-ray spectroscopy (EDX) and temperature programmed desorption (TPD)
- Investigation of the catalytic activity of molybdenum oxide/Al_2O_3-SiO_2 (Mo_rO_q/Al-SSP) catalysts in ethanol dehydration at 1 atm and 200-400^{o}C.

1.4 Research methodology

Part 1

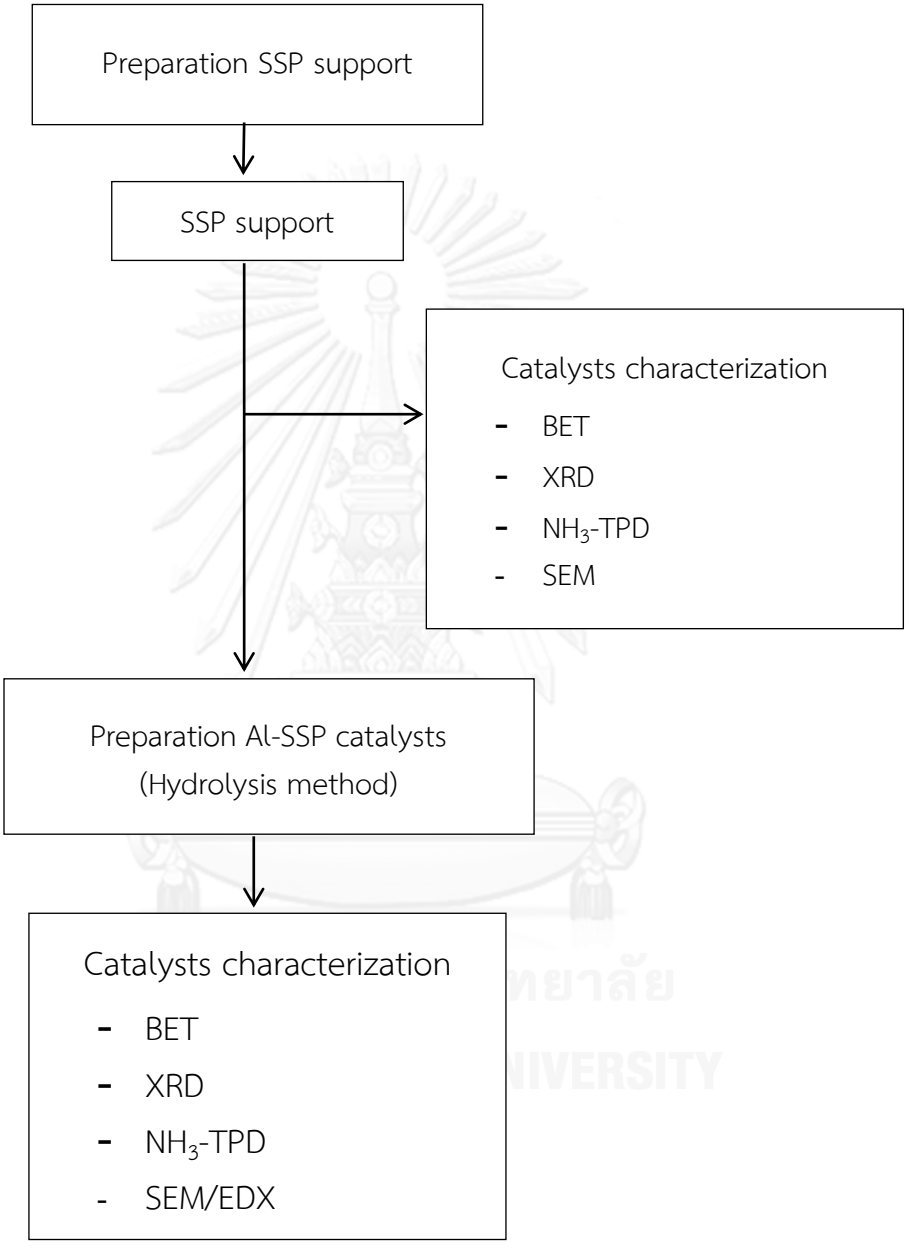

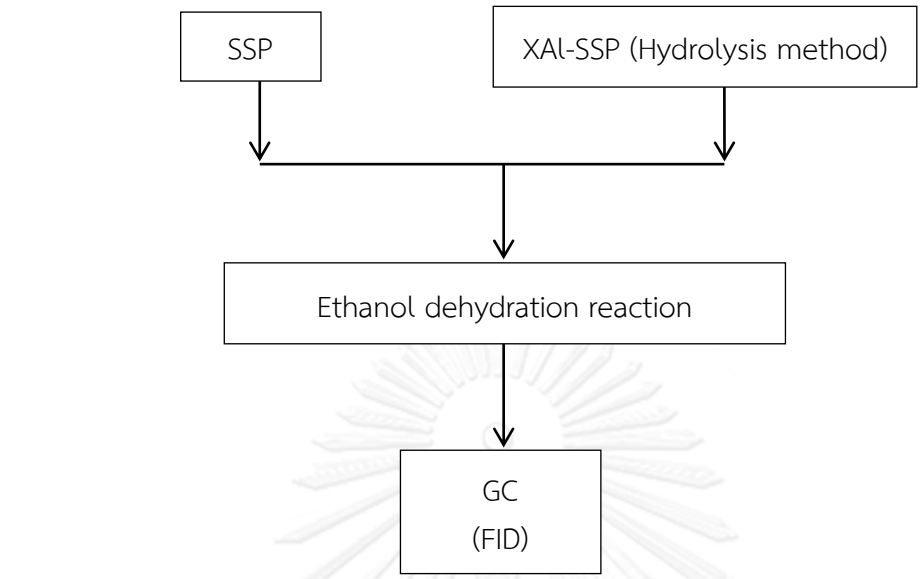
SSP
XAl-SSP (Hydrolysis method)
Ethanol dehydration reaction
GC
(FID)

Part 2

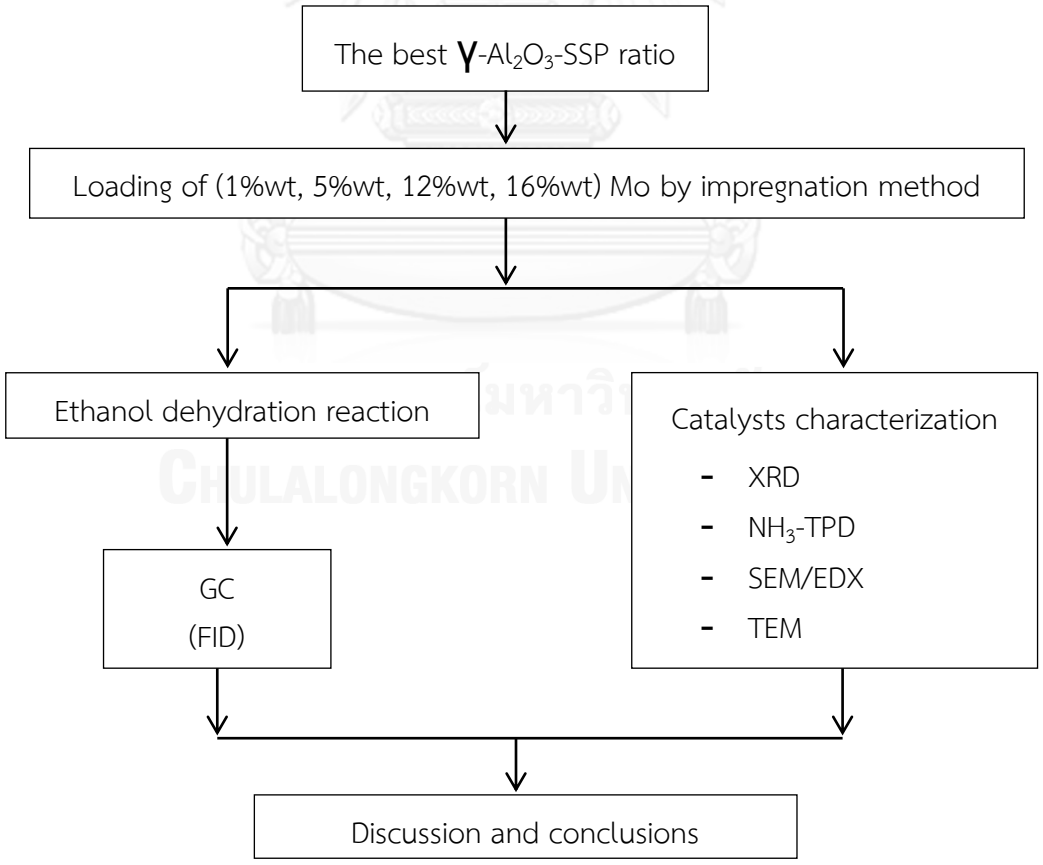
The best γ-Al2O3-SSP ratio
Loading of (1%wt, 5%wt, 12%wt, 16%wt) Mo by impregnation method
Ethanol dehydration reaction
GC
(FID)
Catalysts characterization
- XRD
- NH3-TPD
- SEM/EDX
- TEM
Discussion and conclusions

CHAPTER II

THEORY AND LITERATURE REVIEWS

2.1 Ethanol dehydration reaction

Ethanol dehydration reaction normally distributes ethylene and diethylether as the main products depending on type of active site and operating temperature. However, this reaction has only small byproduct as acetaldehyde [10]. In the past, the steam cracking reaction of hydrocarbons had been widely used for ethylene production. This process can be then replaced by ethanol dehydration reaction because it does not only provide the less complicated process, but also generates the ethylene from biomaterials which are commonly obtained as the wastes from agriculture in Thailand [1, 2]. Ethanol dehydration requires acid catalysts which have been widely used in the industry such as phosphoric acid catalyst, oxide catalysts (Al_2O_3, Al-Si Oxide, Al_2O_3-MgO/SiO_2 etc.), ZSM-5, HZSM-5 [2, 11], SAPO-34, and heteropolyacid catalyst [2]. The mechanism of ethanol dehydration reaction is believed to be the parallel surface reactions or the series reactions. In the parallel surface reactions, ethanol molecules are changed into ethylene molecules together with diethylether molecules. While in the series reaction, molecules of ethanol are converted to diethylether molecules after that changing to ethylene molecules [2]. The mechanism of reactions is shown in **Figure 2.1**.

Ethylene is formed by ethanol dehydration. The temperature, pressure, space velocity, and water content in ethanol are controlled factors of ethanol dehydration [2]. This reaction requires strong acid site or Bronsted acid site [11, 12] and high operating temperature (in the range of 180^{o}C to 500^{o}C) [1]. In order to promote the endothermic reaction [1]. The mechanism of ethanol dehydration is the elimination 1 reaction (E1). Therefore, this reaction requires one ethanol molecule to generate carbocation during the reaction [13]. In the E1, the proton from acid catalyst protonates the hydroxyl group of ethanol molecule to remove the water molecule. After that, the conjugated base of catalyst deprotonates the methyl group and

hydrocarbon rearranging to ethylene [1]. The mechanism of reaction is shown in **Figure 2.2**

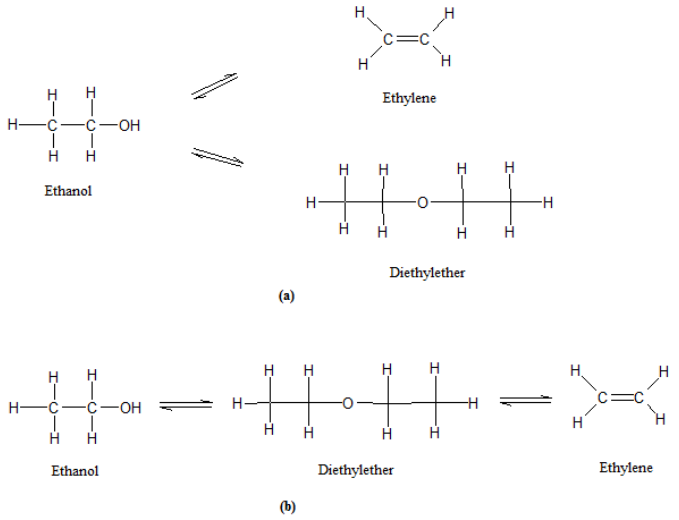

Figure 2. 1 Mechanism of dehydration of ethanol : (a). the parallel reaction and (b). the series reaction [2].

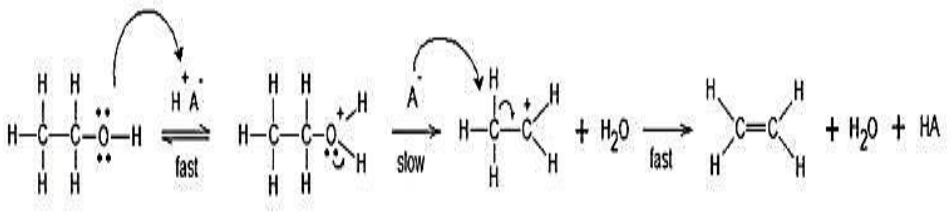

Figure 2. 2 Mechanism of ethanol dehydration to ethylene [1].

The dehydration of ethanol converts ethanol molecules into diethylether. This reaction, which is exothermic, requires weak acid site and low operating temperature (below 240^{o}C) [2]. The mechanism of ethanol dehydration to be diethylether is the second-order nucleophilic substitution reaction (S_N2). Therefore, this reaction requires two ethanol molecules, and no generation of carbocation taking place during the process. In S_N2, the proton from acid catalyst protonates the hydroxyl group of the first ethanol molecule to electrophilic. The lone pair electrons of second ethanol molecule attack the electrophilic of the first ethanol molecule,

and then remove the leaving group [2, 13]. The mechanism of this reaction can be shown in **Figure 2.3**.

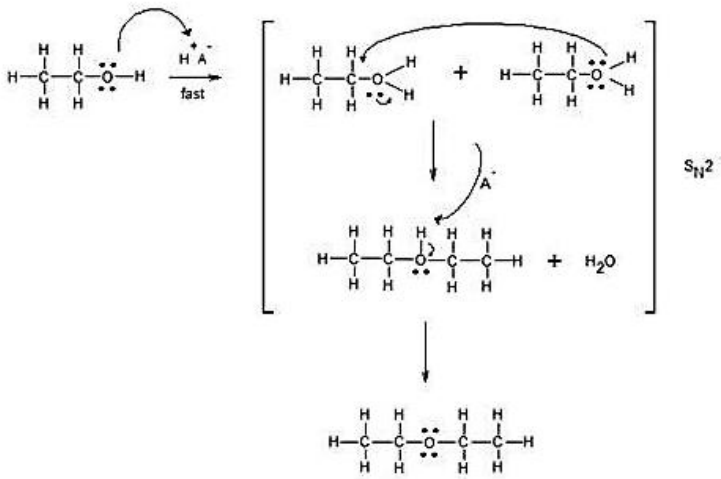

Figure 2. 3 Mechanism of ethanol dehydration to diethylether [2, 13]

2.2 Silica

Silica (SiO_2) is chemical compound consisting of silicon and oxygen, molecular. The operating pressure and temperature driving force are the important factors affecting the structure formation of silica which can be either crystalline or noncrystalline. The silica is formed by nature or synthesis from other precursors.

Silica from soil, rock, animals, and plants is natural silica. For instance, silica in biological system is formed from diatoms of plants and radiolarians of animals. Those fossils are sequentially converted to be diatomite and radiolarite, and then, precipitated in the pond. The sediment of diatomite is used as a filter because of its highly porous. The nature silica normallycontains metal elements as impurities. The structure of this silica is mostly crystalline which consists of quartz, tridymite, and cristobalite, as shown in **Figure 2.4.** The transition phases of silica crystalline depend on temperature as shown in **Figure 2.5** [14].

Figure 2. 4 Crystalline structure of silica [14].

Figure 2. 5 Transition phases of silica crystals [14].

The synthetic silica has many forms such as fiber, sheets, soles, gels, and powder depending upon the application. The structure of synthetic silica is mostly amorphous (noncrystalline). The different forms affected physical properties such as surface area, average pore volume, average pores diameter and pore size. These properties are controlled by synthesis method. The M41S family of synthesized mesoporous silica is mainly used in industry because it has numerous excellent texture properties such as high specific surface area and pore volume, good mechanical and narrow pore size distribution [3, 15]. This family comprises MCM-41, MCM-48, lamella phase (MCM-50) and spherical particles (SSP). They are different forms which are the structure and morphology depending on concentration of ethanol during preparation [16]. The main structure of M41S family has hexagonal, cubic as MCM-41, MCM-48 and lamella phase, but SSP is similar to hexagonal. The morphology of M41S family is shown in **Figure 2.6** [15, 16]. As can be seen from that figure, it illustrates that SSP has an excellent morphology due to the smoothness of spherical particles.

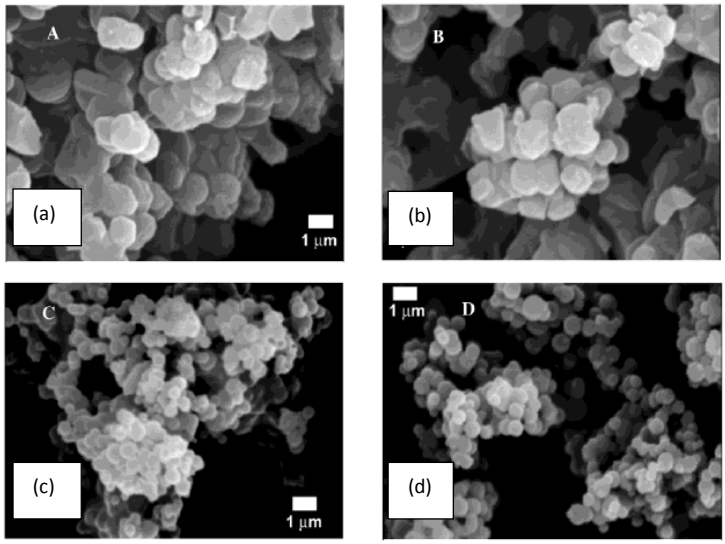

Figure 2. 6 Morphology of M41S silica family: (a) MCM-41, (b) MCM-48, (c) lamella phase and (d) SSP [15].

2.3 Alumina

Alumina or alumina oxide is compound of aluminum and oxygen which has the formula form as Al_2O_3. The alumina was discovered as a material existed in natural clay in 1754 by Marggraf. [17]. The minerals of alumina are corundum and bauxite [18]. The alumina distributes to be three types : corundum, transition phase, and **α**-alumina [18].

The corundum is natural crystalline of alumina. Its appearance represents many colors and transparent such as sapphire (mixed Fe or Ti), ruby (mixed Cr), amethyst (mixed Fe, Mn or Ti). The crystalline structure is alpha-alumina structure as shown in **Figure 2.7** [18, 19].

The alpha-alumina (**α**-Al_2O_3) is regulated by Rankin-Merwin in 1916. This type of alumina can be prepared in two methods. The first method is by heating alumina hydroxide at the temperature above 500 $^{\circ}$C. The other is by heating the transition phase, which is either theta or kappa, at temperature over than 1000 $^{\circ}$C [18]. The

crystalline structure is alpha-alumina structure as the corundum mineral [18]. The **α**-Al_2O_3 is the most stable form of alumina [11] as shown in **Figure 2.7** [18, 19].

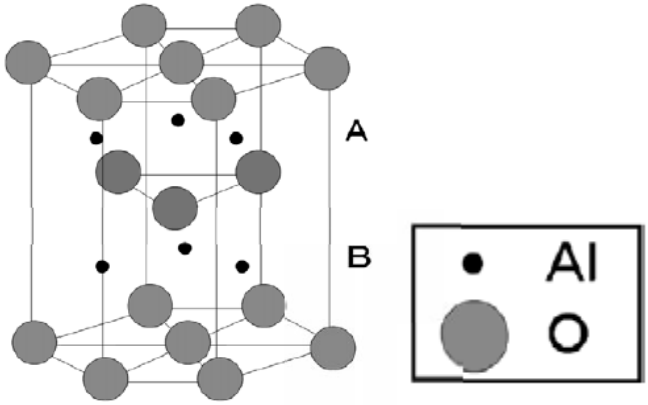

Figure 2. 7 Alpha-alumina structure of corundum mineral and **α**-Al_2O_3 [19].

The transition phases of alumina have seven phases: chi (**K**), kappa (**K**), gamma (**γ**), delta (**δ**), Theta (**θ**), eta (**η**), and alpha (**α**). The transition phases of alumina are produced by heating alumina hydroxide below 1100^{o}C. **Figure 2.8** represents transition phases of alumina after heating by different temperatures. This figure also exhibits the different types of alumina hydroxide affecting to the generation of transition phase at same temperature. Alumina hydroxide has five crystalline structures: gibbsite, bayerite, nordestrandite, diaspora, and boehmite. However, all those structures are called as bauxite [16]. The name of alumina hydroxide depends on molecular form and composition between aluminum and oxygen as shown in **Table 2.1** [19].

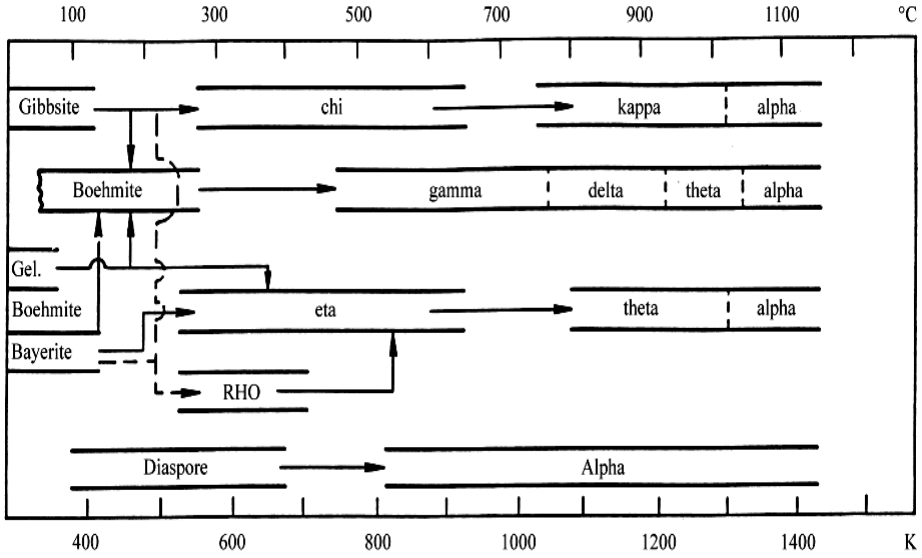

Figure 2. 8 Transition phases of alumina [18].

Table 2. 1 Types of bauxite [19].

Mineral Name	Chemical Composition	Accepted Standard Crystallographic Designation (1957)	Alcoa (1930)
Gibbsite / Hydrargillite	Aluminum trihydroxide	γ-$Al(OH)_3$	Alpha alumina trihydrate
Bayerite	Aluminum trihydroxide	α-$Al(OH)_3$	Beta alumina trihydrate
Nordstrandite	Aluminum trihydroxide	$Al(OH)_3$	
Boehmite	Aluminum oxide hydroxide	γ-AlOOH	Alpha alumina monohydrate
Diaspore	Aluminum oxide hydroxide	α-AlOOH	Alpha alumina monohydrate

The acidity and basicity of alumina can be alternated due to the existence or distinction of hydroxyl group from water molecules. The position of acidity is assigned by H_2O molecules coordinated with cationic sites and Al^{3+} ions, whereas the basicity is defined by O^{2-} anion vacancies and hydroxyl group [4]. The water molecules in alumina are removed by heat, calcination, generation of Lewis acid site and basic site. Whereas by adding water molecules as pretreated catalyst, Lewis acid site is changed to be the weak Bronsted acid site [20, 21]. The mechanism of alumina acidity is illustrated in **Figure 2.9** [20].

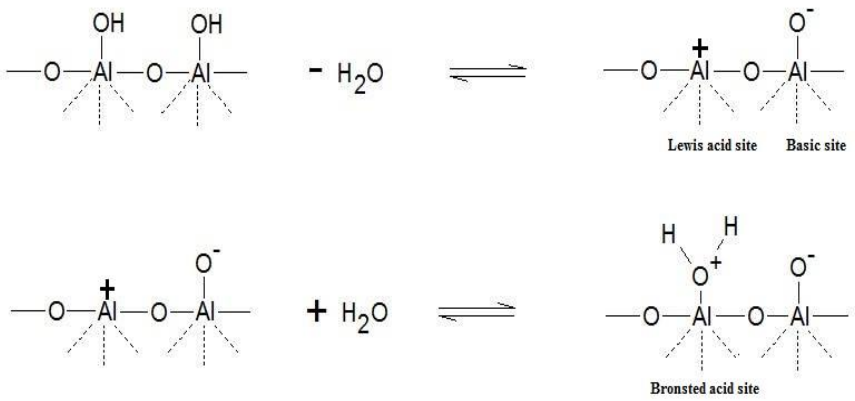

Figure 2. 9 Mechanism of alumina acidity [20].

Alumina is used as commercials catalysts or support in many industrial processes. The using alumina in catalyst field provides excellent high degree of metal dispersion, moderate high surface area, and thermal stability over wide range temperature [21].

2.4 Alumina-silica composite.

The alumina-silica composite is used as a support or catalyst [22] depending on required active site of reaction. This composite catalyst is bifunctional catalysts containing mostly acid site presented on its surface. [22]. Nowadays, this composite, which can also be called as acid catalyst, has been widely used in petroleum and chemical industries [10, 23]. The acidity of alumina-silica is analyzed by FT-IR pyridine adsorption or NH_3-TPD techniques. The FT-IR pyridine adsorption technique refers to Bronsted and Lewis acid site, while the NH_3-TPD technique quantify the amount of weak, medium, and strong acid site which relies on range of temperature. These techniques can be used to determine the efficiency of active site for reaction, especially ethanol dehydration to ethylene which requires strong acid site or Bronsted acid site [11, 12]. The structure of alumina-silica composite is formed by substitution of Al^{3+} to Si^{4+} in silica network [22] during calcination step. In this process, the aluminium and silica, which has six-coordinate and four-coordinate, respectively, generates negative charge. Therefore, adding proton to this structure in order to form

Bronsted acid site is needed. However, some parts of its structure can also generates dehydroxylation which can remove hydroxyl group resulting in the formation Lewis acid site [22]. The ^{27}Al NMR technique provides the determination of the aluminium atoms in alumina-silica composite, which contains tetrahedral, pentahedral, and octahedral as aluminium atoms in silica network, interface between aluminium atoms with silica surface, and cluster of aluminuim oxide, respectively [24]. As mentioned above, the amount of Bronsted acid site of catalysts depends upon the amount of tetrahedral aluminium in silica structure [25]. The alumina-silica composites have more acid site than alumina and silica. Hence, it is well compatible with the ethanol dehydration more than pure oxides (alumina and silica) mentioned by [26]. The acidity of composite catalysts is stronger than pure oxide catalysts as shown in ref. [27]. The aluminium over silica catalyst or silicon over alumina catalyst has amount of Bronsted acid site more than γ-Al_2O_3, but has less amount of Lewis acid site than γ-Al_2O_3. The acidity of catalysts is dependent upon the amount of aluminium in catalysts and calcination temperature [22, 24]. The ref. [21] cited that the alumina-silica mixed oxide provides higher protonic acidity degree than single oxide.

2.5 Molybdenum

Molybdenum was pierced in 1778 by Carl Wilhelm Scheels [28]. The appearence of this metal is silvery gray as shown in **Figure 2.10** . Molybdenum is used in many applications such as a compound of alloys, mineral of plants (cauliflower), cofactor of enzymes in humans and animals for metabolism fats and carbohydrates [29]. Molybdenum is a catalyst in industry used for pollution controls (NO_2/NO_x) [30].

Figure 2. 10 The feature of molybdenum metal [29].

Molybdenum is the 42nd element in periodic table, between niobium and technetium. The electronic structure of molybdenum is [Kr] 5s^{1} 4d^{5}. The crystalline structure is body-centered cubic (bcc), and lattice parameters are a = b = c = 314.7 pm [31]. The physical properties of molybdenum are shown in **Table 2.2** and the crystalline structure is shown in **Figure 2.11**

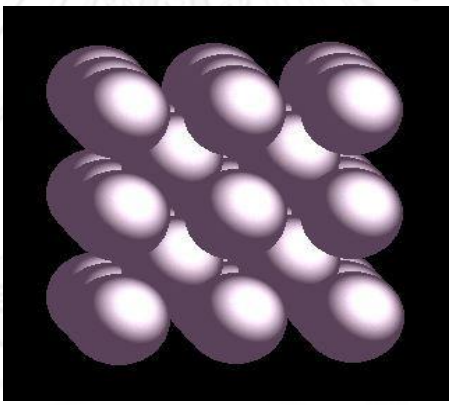

Figure 2. 11 The crystalline structure of molybdenum [31].

Table 2. 2 The physical properties of molybdenum

Property	Value
Element category	Transition metal
Atomic number	42
Atomic weight	95.94
Melting point	2623^{o}C
Boiling point	4639^{o}C
Electrical resistivity	53.4 nΩ. M (at 20^{o}C)
Thermal conductivity	138 w/m.K
Young's modulus	329 GPa

Many industries use molybdenum to accelerate chemical reaction. The compound of molybdenum has many forms which are suitable for various reactions such as the using molybdenum diselenide ($MoSe_2$) and molybdenum ditelluride ($MoTe_2$) in superconducting thin film industry [32], using molybdenum pentachloride and molybdenum hexacarbonyl in the electronics industries and in chemical vapor deposition [33], using Fe-Mo oxide in the methanol oxidation reaction, using Mo oxide on alumina in the metathesis of olefin, [34] and using MoO_3/Al_2O_3 or MoO_3/SiO_2 or MoO_3/Al_2O_3-SiO_2 in the hydrotreating or hydrocracking process [35]. The MoO_3 has good dispersion ability on Al_2O_3 supports [35]. The molybdenum onto silica-alumina generates new Bronsted acid site and reduced Lewis acid site more than cerium and nickel [36]. The calcination temperature affects to molybdenum species and distribution on support [37]. Numerous previous works relating to MoO_3/Al_2O_3-SiO_2 show that adding molybdenum onto Al_2O_3-SiO_2 catalysts influences the activity of reaction which requires acid site. This is because molybdenum generates new Bronsted acid site and decreases Lewis acid site. An increase in the amount of MoO_3 over alumina rich-support provides many new Bronsted acid sites [35, 38]. The silica rich-supported has B/L maximum ratio of 2%MoO_3 [38]. The Mo oxide on Al_2O_3 is formed as monolayer, but Mo atom size is less than 5 atom/nm^2 because interaction between Mo oxide and support is strong. The structure of Mo oxide on SiO_2 could be

tetrahedral, octahedral, and MoO_3. The formed structure is independent on the number of Mo atoms [25].

CHAPTER III

EXPERIMENTAL

3.1 Catalyst preparation

3.1.1 Chemicals

The chemicals used in the catalyst preparation are shown in **Table 3.1**

Table 3. 1 The chemicals used for synthesis

.

Chemicals	Supplier
Tetraethoxysilane 98% (TEOS)	Aldrich
Aluminium isopropoxide 98% ($Al(OP^{i})_3$)	Aldrich
Cetyltrimethylammonium bromide (CTAB)	Aldrich
Ammonia 30%	Panreac
Ethanol 99.99%	J.T. Baker
Isopropanol	Merck
Ammonium heptamolybdate-tetrahydrat	Merck
De-ionized water	

3.1.2 Synthesis of the spherical silica particle (SSP) [4]

First, the spherical silica particle (SSP) support was prepared following molar ratio: 1TEOS: 0.3CTAB: 11NH_3: 58Ethanol: 144H_2O [3]. Secondly, this solution was stirred at room temperature for 2 hours. After that, the white precipitate was separated from solvent by centrifuge. Then, the sample was dried at 110^{o}C overnight and was calcined in air at 550^{o}C for 6 hours.

3.1.3 Synthesis of the Al2O3-SSP composites support [4]

The SSP was added into the solution (desired ratio of aluminium isopropoxide: 2-propanol) and was stirred for 1 hour at room temperature. Then, adding ammonia [H_2O:$Al(OPr^1)_3$ = 4:1] into the sample for hydrolysis and was stirred at room temperature for 20 hours. After that the sample was dried at 110^{o}C for 24 hours. Dried sample was calcined in air at 650^{o}C for 2 hours.

3.1.4 Synthesis of the Mo oxide/Al_2O_3-SSP

The Mo oxide/Al_2O_3-SSP catalysts were prepared by incipient wetness impregnation method. First, the desired amount of ammonium heptamolybdate-tetrahydat, which is a precursor of molybdenum was dissolved in DI water. Secondly, this solution was dropped into Al_2O_3-SSP composites support after that the catalyst was dried at 110^{o}C for 4 hours in oven and calcined in air at 550^{o}C for 4 hours.

3.1.5 Nomenclature of catalysts

In this research, the catalyst samples used the nomenclature as follows:

- **XAl-SSP** refers to Al_2O_3-SSP composites support.
- **YMoAl-SSP** refers to molybdenum supported over Al_2O_3-SSP composites support.

X refer to the weight of Al_2O_3

Y refer to the weight of molybdenum

3.2 Characterization of catalysts

3.2.1 N_2-physisorotion

The surface area, pore volume and pore diameter of catalysts were determined by nitrogen gas adsorption at liquid nitrogen temperature (-196°C) using Micromeritics ChemiSorb 2750 Pulse chemisorption System instrument. Before the experiment, the sample was thermally treated at 150°C for 3 hours.

3.2.2 X-ray diffraction (XRD)

The bulk crystal structure and X-ray diffraction (XRD) patterns of all catalysts were measured by the SIEMENS D5000 X-ray diffractometer connected with a computer with Diffract ZT version 3.3 programs for fully control of the XRD analyzer. The experiments were carried out by using CuK_α radiation with Ni filter in the 2θ range of 10 to 90 degrees with a resolution 0.02°.

3.2.3 Scanning Electron Microscope (SEM) and Energy X-ray Spectroscopy (EDX)

The morphology and elemental dispersion over the catalysts surface were determined by scanning electron microscope (SEM) and energy x-ray spectroscopy (EDX), respectively. The SEM model is JEOL mode JSM-5800LV and Link Isis Series 300 program was perform for EDX.

3.2.4 Temperature Programmed Desorption (TPD)

The acid properties of all catalysts were measured by temperature programmed adsorption of ammonia (NH_3-TPD) equipment by using micromeritics chemisorp 2750 Pulse Chemisorption System. The catalyst samples were pretreated at 400°C in a flow of helium. The sample was saturated with 15%NH_3/He at 120°C for 1 hour. After saturation, the physisorbed ammonia was desorped in a helium gas flow. Then, the sample was heated from 30 to 800°C at a heating rate of 10°C /min. The amount of ammonia in effluent was measured via TCD signal as a function of temperature.

3.2.5 Transmission Electron Microscope (TEM)

The molybdenum particle distribution of all catalysts was observed by using JEOL-JEM 200CX transmission electron microscope operated at 200 kV.

3.3 Reaction study in ethanol dehydration

3.3.1 Materials

In this experiment, about 0.05 g of catalyst was packed in fix-bed down flow reactor at atmosphere pressure. A carrier gas (argon) was fed into the reactor for pretreat the catalyst for 1 hour. Ethanol in liquid phase was saturated for 1 hour at 200^{o}C, and it was fed into the reactor. The effluent products were collected at 200^{o}C, 250^{o}C, 300^{o}C, 350^{o}C and 400^{o}C .

3.3.2 Instruments and apparatus

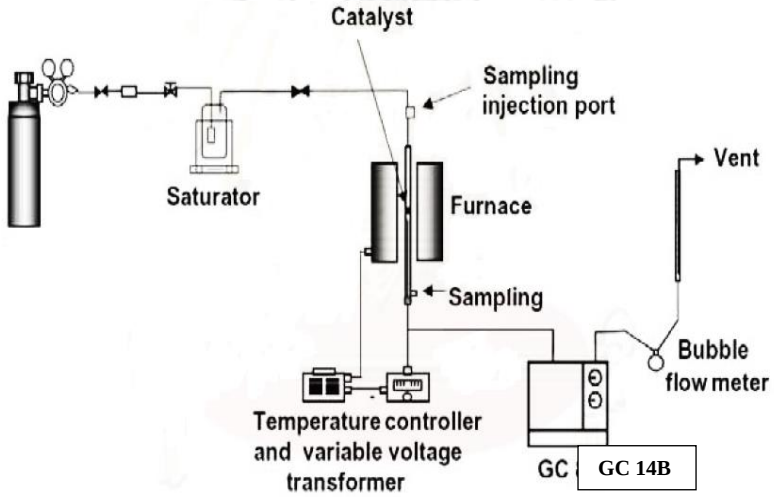

Figure 3. 1 Flow diagram of ethanol dehydration system

The flow diagram of ethanol dehydration is shown in **Figure 3.1**. The main instruments and apparatus in the reaction study are explained as follows:

- **Saturator**

  The saturator is equipment to vaporize ethanol inyo liquid phase to saturated ethanol.

- **Reactor**

  The reactor made from a borosilicate glass tube (O.D. 9” and length 12 cm.).

- **Electrical furnace**

  The furnace supplied heat to the reactor. The reactor was operated from room temperature up to 400^{o}C at 190 volt of voltage.

- **Temperature controller and variable voltage transformer**

  The variable voltage transformer and solid state relay temperature controller connected to thermocouple for measurement and adjustment the temperature of catalysts in the reactor.

- **Gas chromatograph**

  The composition in the product stream was analyzed by gas chromatograph with a flame ionization detector, Shimadzu GC14B (DB-5). The operating condition for this instrument is shown in **Table 3.2**

3.3.3 Procedure

1. 0.01 g of quartz wool was placed into the middle of borosilicate glass reactor after that the amount of catalysts about 0.05 g was packed on quartz wool.

2. The reactor was located in the electrical furnace then opening the argon gas flow into the reactor and adjustment voltage and temperature controller up to 190 volt and 200^{o}C, respectively for pretreat the catalysts for 1 hour. A flow rate of argon gas is 50 ml/min.

3. Ethanol in liquid phase was saturated for 1 hour at 200^{o}C by 50 ml/min of argon gas, and it was fed into the reactor.

4. The effluent products were analyzed by gas chromatography with flame ionization detector.

Table 3. 2 Operating conditions for gas chromatograph

Gas Chromatography	**Shimadzu GC-14A**
Detector	FID
Capillary column	DB-5
Carrier gas	Nitrogen (99.99 vol.%)
	Hydrogen (99.99 vol.%)
Column temperature	
▪ Initial	40 °C
▪ Final	40 °C
Injector temperature	150 °C
Detector temperature	150 °C
Time analysis	12 min
Analyzed gas	Ethylene
	Acetaldehyde
	Ethanol
	Diethyl ether

CHAPTER IV

RESULTS AND DISCUSSION

This chapter mentioned investigation characteristic and catalytic activity of spherical silica particle, alumina-silica composite and alumina-silica composite-supported molybdenum catalysts in ethanol dehydration reaction. This chapter is distinguished into two parts. The first part illustrated characteristic and activity of spherical silica particle and alumina-silica composite catalysts. The characteristic and activity alumina-silica composite-supported molybdenum catalysts are exhibited in the last part.

4.1 Characterization and catalytic activity of spherical silica particle (SSP) and alumina-silica composite catalysts (Al-SSP).

This section exhibited the characteristic of spherical silica (SSP) and alumina-silica composite catalysts (Al-SSP) from various techniques such as BET surface area, X-ray diffraction, scanning electron microscopy (SEM), energy dispersive X-ray spectroscopy (EDX), temperature programmed desorption of ammonia (NH_3-TPD). In the last section, it presented activity of all catalysts in ethanol dehydration reaction.

4.1.1 Nitrogen physisorption

The nitrogen physisorption technique was used to determine the surface area, average pore diameter, average pore volume, isotherm and pore size distribution of spherical silica particle (SSP) and alumina-silica composite catalysts (Al-SSP) having various compositions between alumina and silica.

Table 4.1 summarizes results of surface area, average pore diameter and average pore volume of all catalysts. It reveals that the surface area of pure spherical

silica particle was the highest whilst those of composite catalysts were significantly decreased by increasing the amount of alumina. There was concordance with further of average pore diameter which was increased. The average pore diameter was ranged from 2.35 to 6.39 nm. Furthermore, the results of isotherm in **Figure 4.1** indicates that they were identical, so it was said that all catalysts are mesopore type catalyst. **Figure 4.2** presents the pore size distribution of all composite catalysts, it can be observed that the amount of alumina was not affect on the distribution of pore size in all composite catalysts.

Table 4. 1 The surface area, average pore diameter and average pore volume of spherical silica particle and alumina-silica composite catalysts

Catalysts	Surface area (m^2/g)	Average pore diameter (nm.)	Average pore volume (cm^3/g)
SSP	1133	2.35	0.73
20Al-SSP	684	2.68	0.59
40Al-SSP	454	4.04	0.54
60Al-SSP	443	5.93	0.81
80Al-SSP	367	6.39	0.76

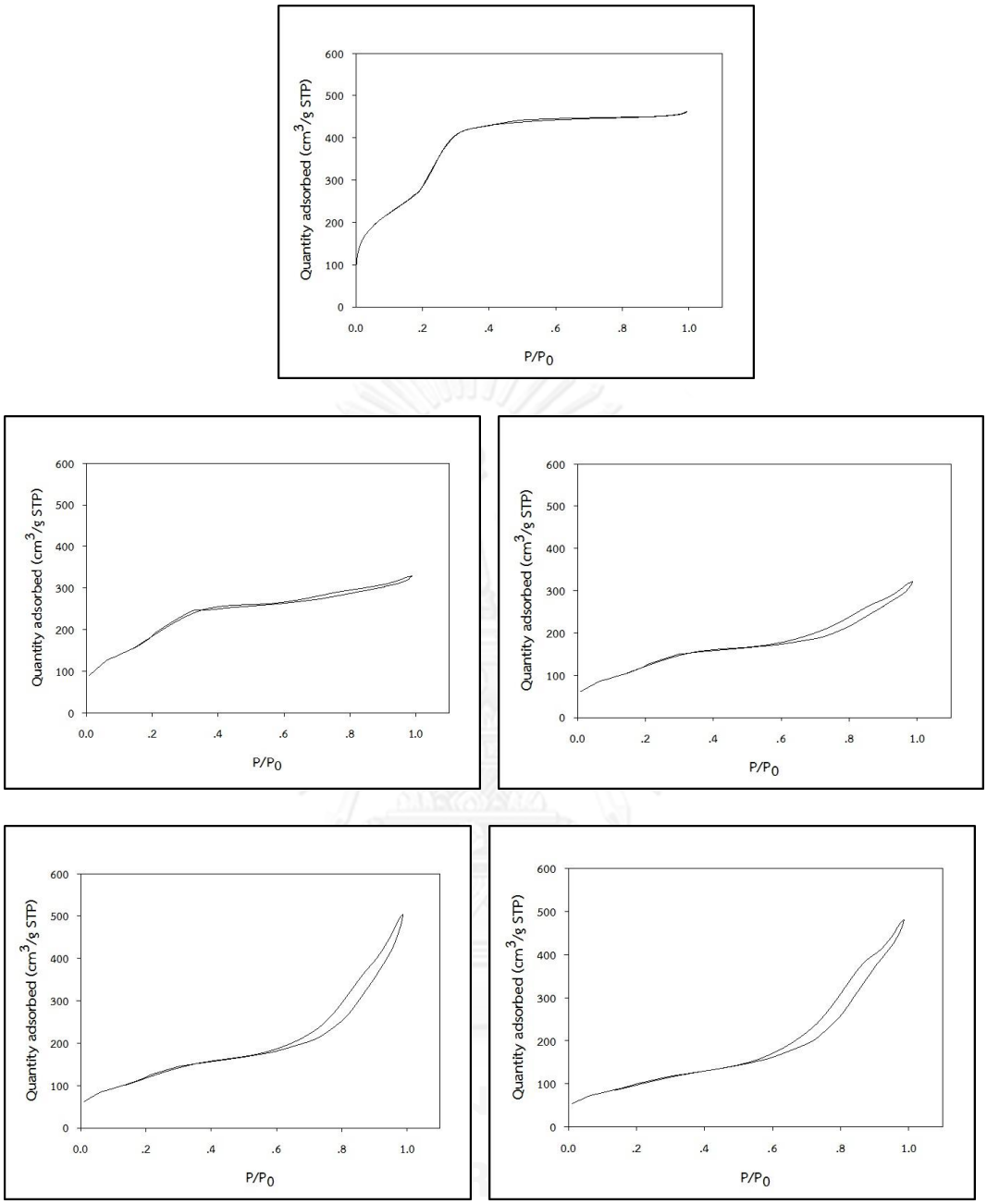

Figure 4. 1 The adsorption-desorption isotherms of all catalysts ; (a) SSP, (b) 20Al-SSP, (c) 40Al-SSP, (d) 60Al-SSP and (e) 80Al-SSP

.

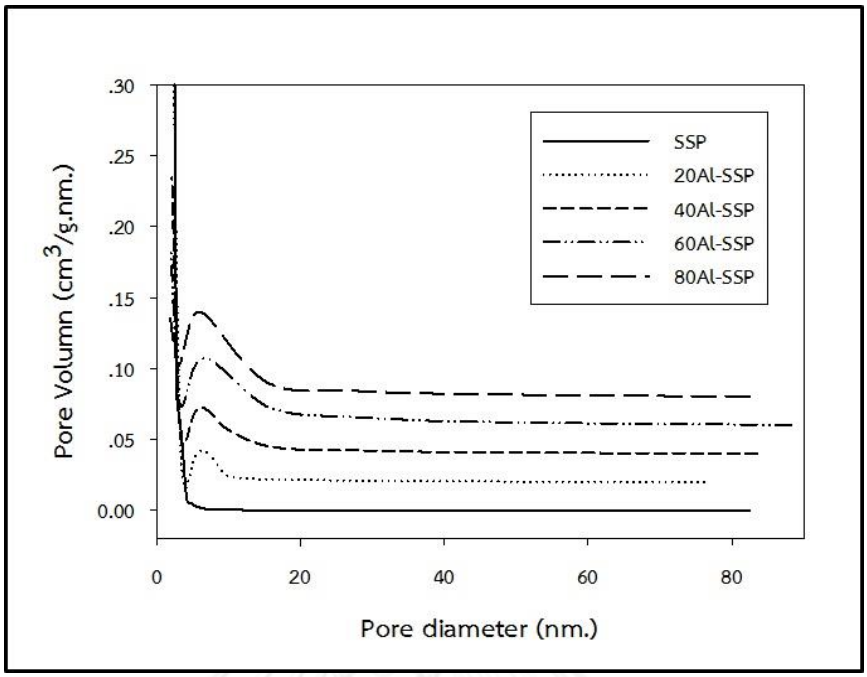

Figure 4. 2 The pore size distribution of all composite catalysts

4.1.2 X-ray diffraction

The X-ray diffraction technique is established chemical phase composition and bulk crystal of crystalline material having crystal size more than 3-5 nm. The diffraction angles (2θ) were used between 10^{o} and 90^{o} for analysis.

XRD patterns of spherical silica particle (SSP) and alumina-silica composite catalysts (Al-SSP) with various compositions between alumina and silica are shown in **Figure 4.3.** The XRD patterns of SSP present only amorphous silica having board peaks around 21-24^{o}. Moreover, the maximum sharp peaks center at 45^{o} and 67^{o} of all composite catalysts was observed indicating the presence of γ-Al_2O_3 crystallite. These peaks were distincted when adding alumina more than 40 weight percent as seen in 40Al-SSP, 60Al-SSP and 80Al-SSP. On the other hand, board peaks of all composite catalysts were decreased by loading alumina.

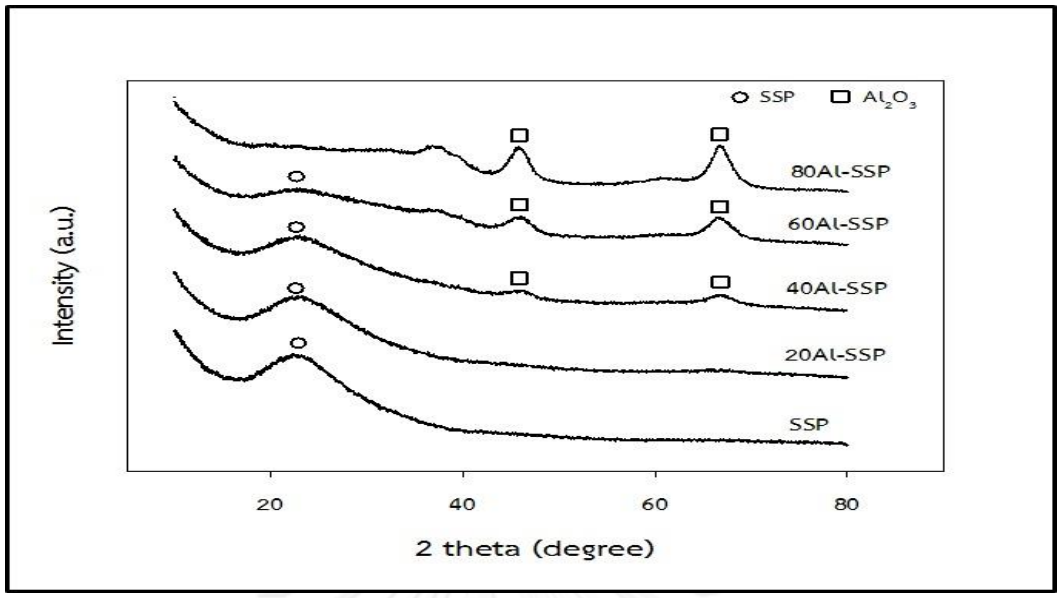

Figure 4. 3 The XRD patterns of all catalysts

4.1.3 Scanning electron microscopy (SEM)

The morphology of spherical silica particle (SSP) and all composite catalysts (Al-SSP) was investigated by scanning electron microscopy (SEM). The images of spherical silica particle (SSP) and all composite catalysts (Al-SSP) are illustrated in **Figures 4.4 and 4.5**, respectively.

Figure 4.4 shows that the morphology of silica was spherical with average size of ~ 0.5 μm. The morphology of all composite catalysts was changed from spherical particle to cluster after adding alumina over silica particles and heated that alumina particle covered on silica particles as shown in **Figure 4.5.**

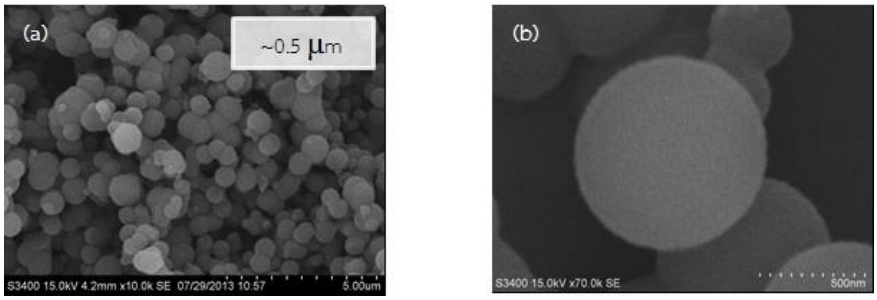

Figure 4. 4 The SEM micrograph of SSP

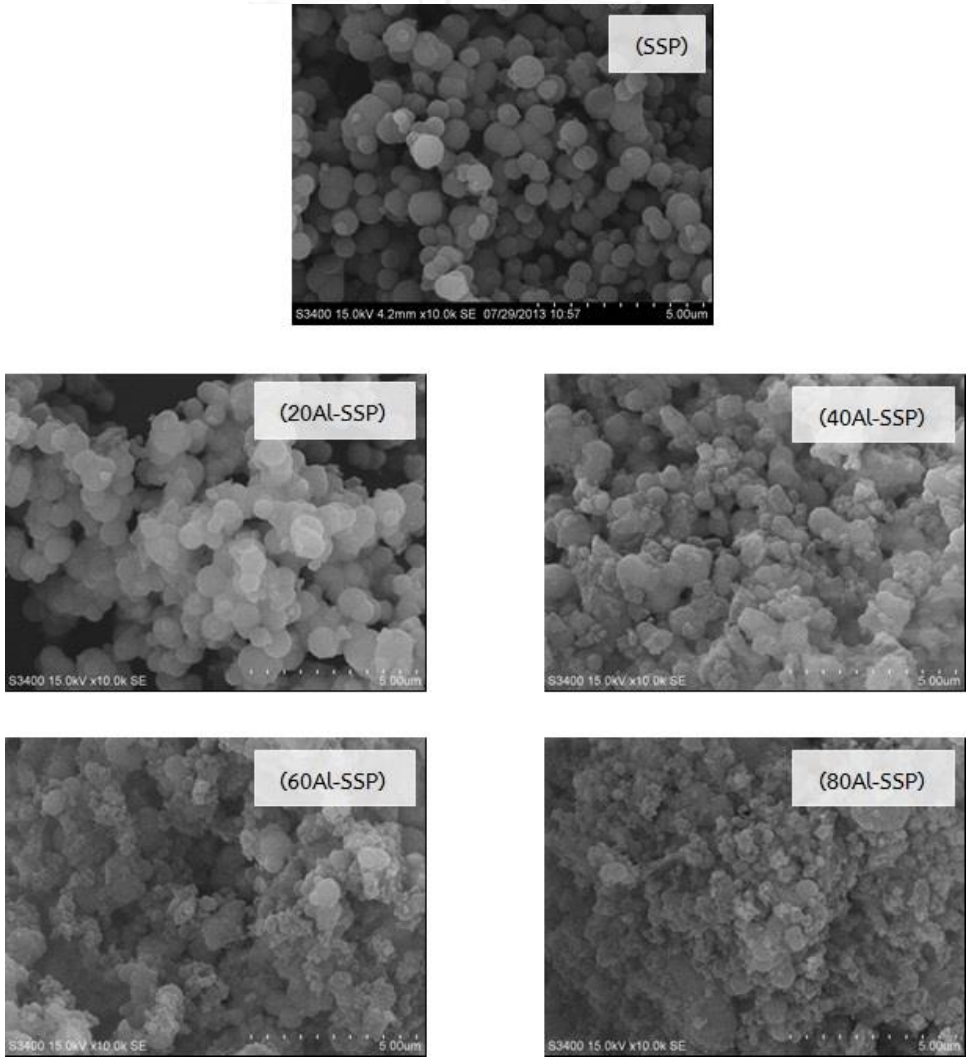

Figure 4. 5 The SEM micrograph of all composite catalysts

4.1.4 Energy dispersive X-ray spectroscopy (EDX)

The elemental distribution of catalysts, spherical silica particle (SSP) and all composite catalysts (Al-SSP), was studied using energy dispersive X-ray spectroscopy (EDX).

The EDX mapping of all catalysts is displayed in **Figures 4.6 to 4.10.** The concentration of alumina, silica and oxygen distribution on outer surface of all catalysts is represented with the white granule. It is suggested that alumina covering on the surface of spherical silica particle was uniform and well distribution.

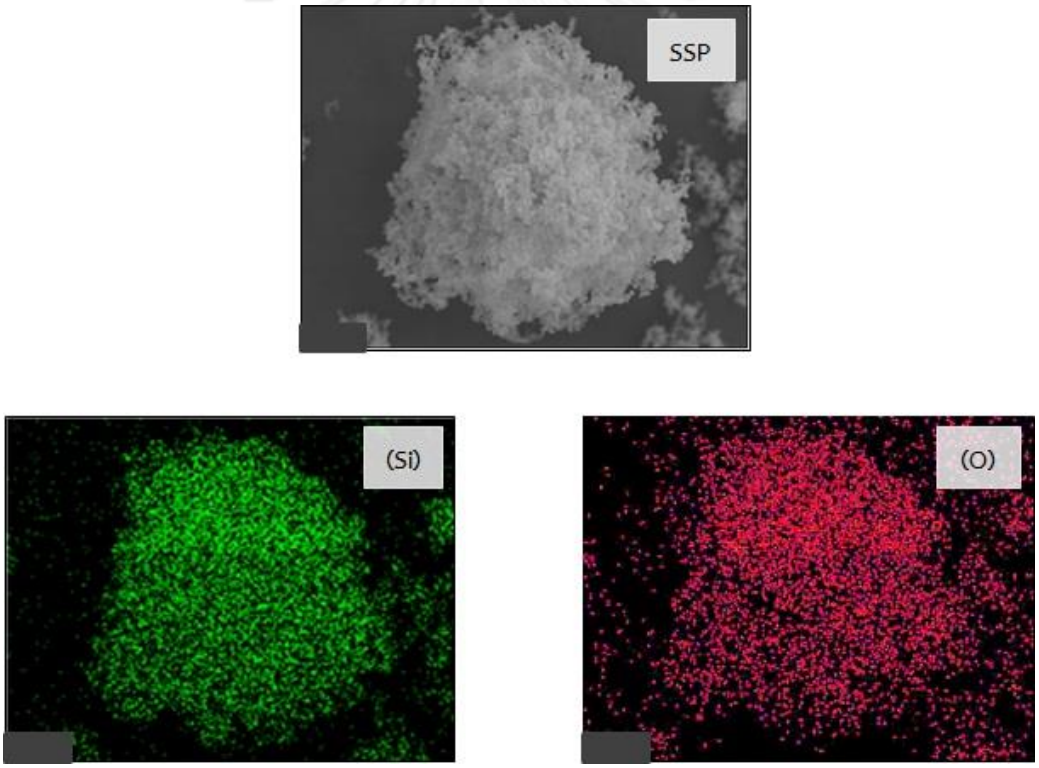

Figure 4. 6 The EDX mapping of SSP

.

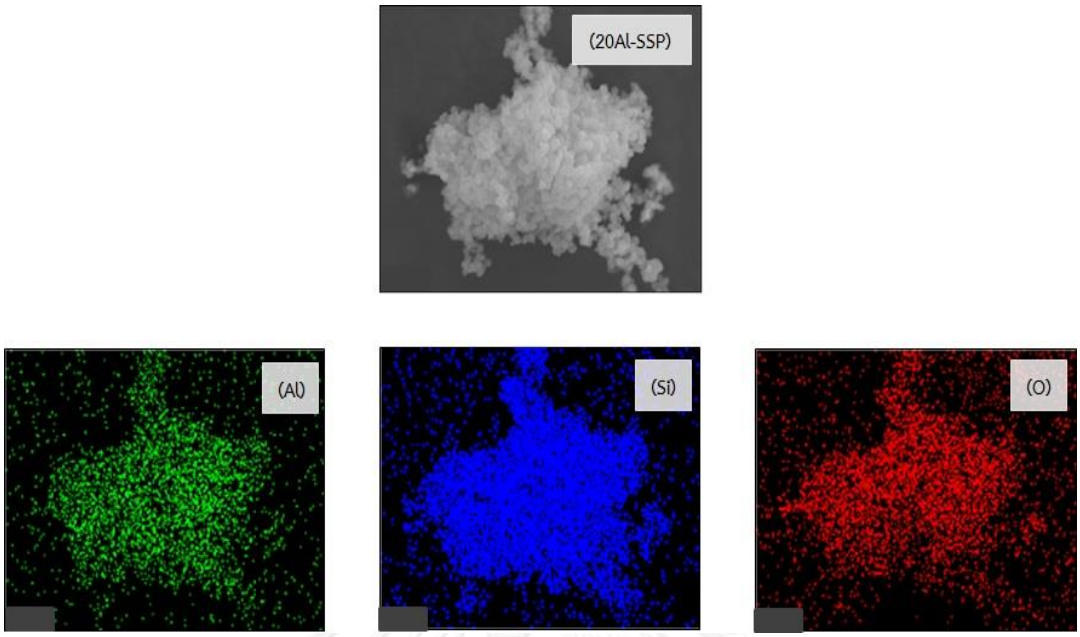

Figure 4. 7 The EDX mapping of 20Al-SSP

.

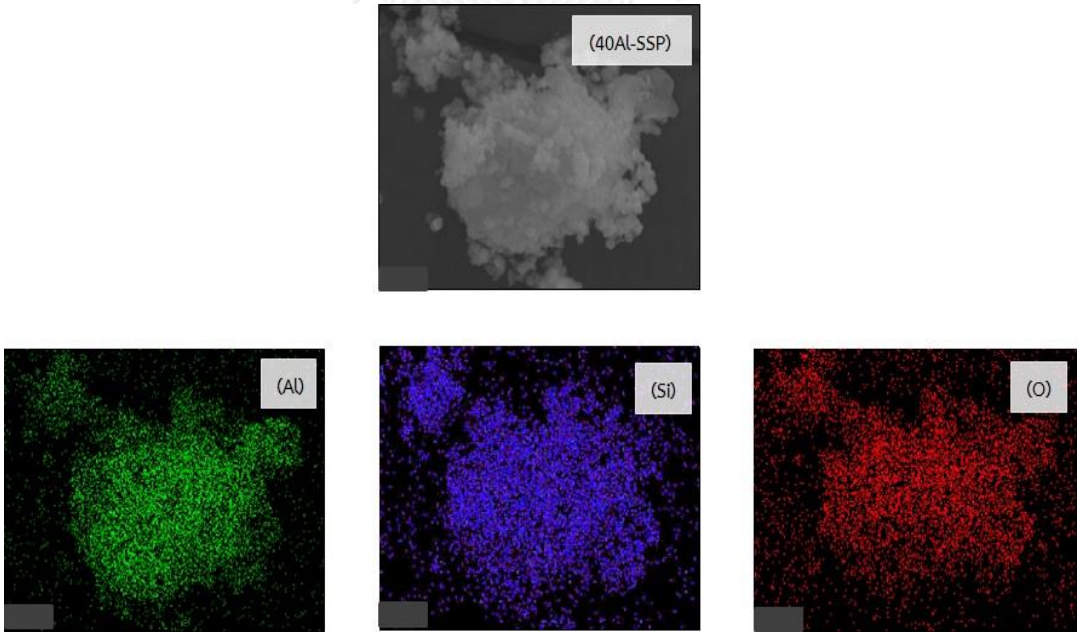

Figure 4. 8 The EDX mapping of 40Al-SSP

.

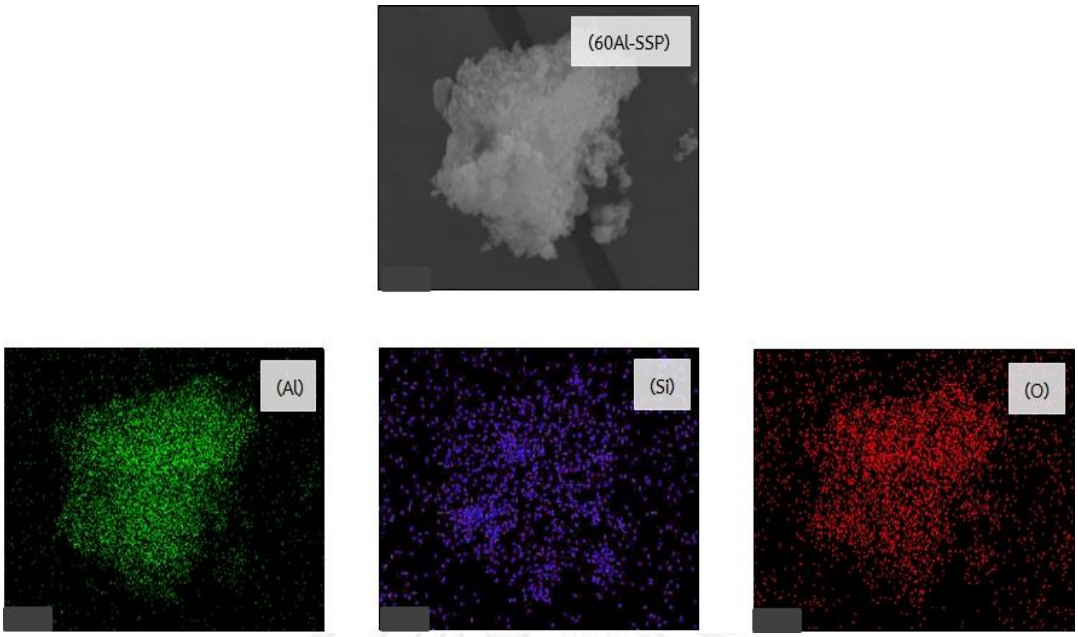

Figure 4. 9 The EDX mapping of 60Al-SSP.

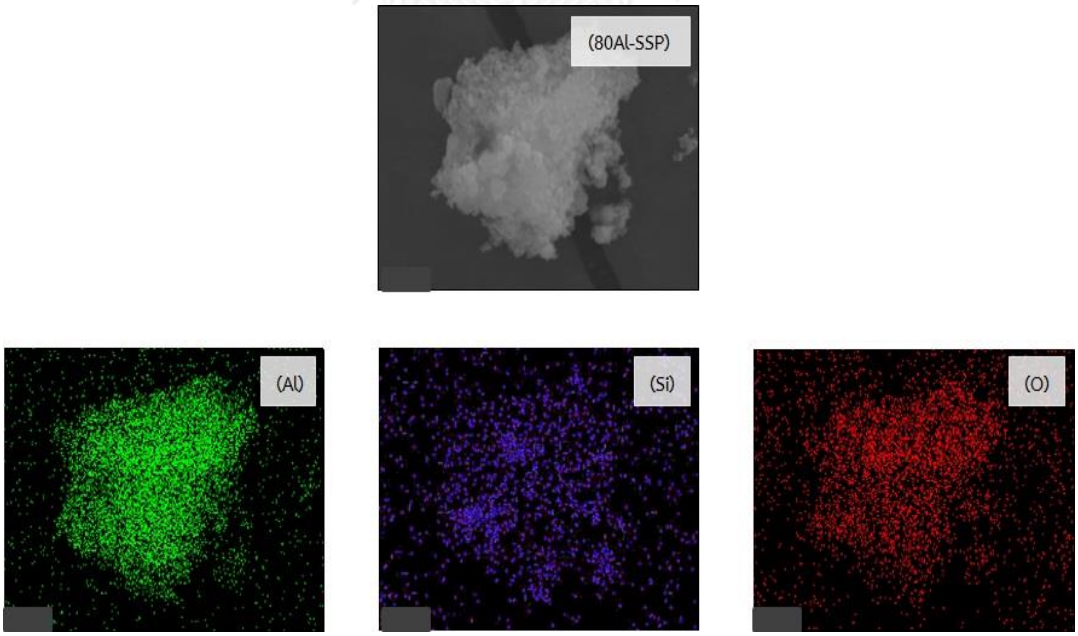

Figure 4. 10 The EDX mapping of 80Al-SSP

.

The composition of catalysts was analyzed from EDX as shown in **Table 4.2**. The amount of oxygen on the surface of all catalysts has been coincidental. In part of alumina, the concentration increased by adding alumina, excepting of the 80Al-SSP which decreasing amount of alumina due to some of alumina inserted in interior of silica particle. The amount of silica decreased due to conceal with alumina particle.

Table 4. 2 The amount of elemental distribution on surface SSP and all composite catalysts.

Catalysts	Amount of weight on surface (wt%)		
	Al	Si	O
SSP	-	54.84	45.16
20Al-SSP	11.79	34.31	53.90
40Al-SSP	28.84	20.14	51.02
60Al-SSP	40.58	7.51	51.90
80Al-SSP	37.90	8.56	53.54

4.1.5 Temperature programmed desorption of ammonia

The amounts of weak acid sites, medium-strong acid sites and total acid sites of all catalysts were detected by temperature programmed desorption of ammonia (NH_3-TPD). The sample was heated from 30 to 800^{o}C at a heating rate 10^{o}C /min.

Table 4.3 shows the acid properties of all catalysts. The number of weak acid sites and medium-strong acid sites on SSP support was the lowest when compared with other catalysts. As considering all composite catalysts, the amount of weak acid sites increased after loading of alumina onto spherical silica, but the 60Al-SSP was the lowest when compared with other composite catalysts. Moreover, the increasing of alumina affected on increasing the number of medium-strong acid sites. Therefore, the 60Al-SSP had the highest, but the 80Al-SSP had the lowest in all composite catalysts. The total acid site was ranged from 0.65 to 2.05 mmole/g.cat. The amount of alumina influenced the acidity of catalysts.

Table 4. 3 The amount of acid site of SSP and all composite catalysts.

Catalysts	Number of acid site (mmole/g.cat)		
	Weak	Medium-strong	Total
SSP	0.00	0.65	0.65
20Al-SSP	0.51	1.29	1.80
40Al-SSP	0.69	1.36	2.05
60Al-SSP	0.25	1.45	1.70
80Al-SSP	0.77	1.22	1.99

4.1.6 Catalytic activity of spherical silica particle (SSP) and alumina-silica composite catalysts (Al-SSP) in ethanol dehydration reaction.

The catalytic activity of spherical silica particle (SSP) and alumina-silica catalysts (Al-SSP) in ethanol dehydration reaction was indicated by the ethanol conversion and selectivity of products. The procedure of investigation performance catalysts: Firstly, the moisture containing in the catalysts was removed at 200^{o}C in carrier gas flow 50 ml/min for 1 h. After that saturated liquid ethanol by saturator in carrier gas flow 50 ml/min for 1 h. was flowed the saturated into a fixed bed reactor for reaction. The resulted reaction is displayed in **Figure 4.11** to **Figure 4.14.**

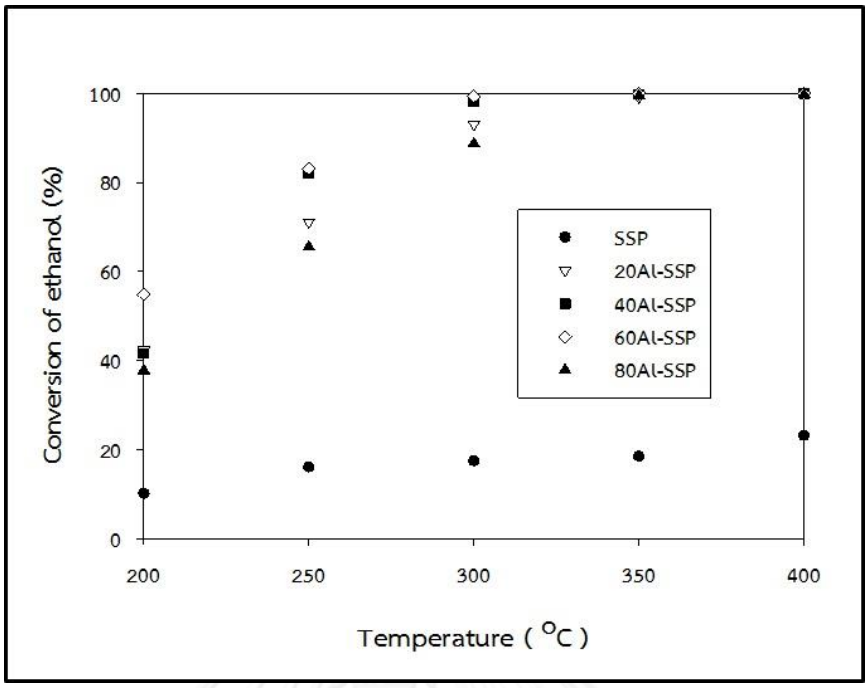

Figure 4. 11 The ethanol conversion at different temperatures of all catalysts

The conversion of ethanol dehydration reaction is displayed in **Figure 4.11.** The result indicates that the ethanol conversion of each catalysts depended on the reaction temperature. Increased temperature gave higher conversion. As regarding the low temperature, 200-300^{o}C, it was found that the 60Al-SSP gave evidently the highest conversion. This result agreed with amount of medium-strong acid sites measured by NH_3-TPD method. So, it can be predicted that the ethanol conversion depended on the amount of medium-strong acid sites. At temperature ~ 350^{o}C, the ethanol conversion of all composite catalysts went up to 100 percent but, the SSP still exhibited the lowest conversion.

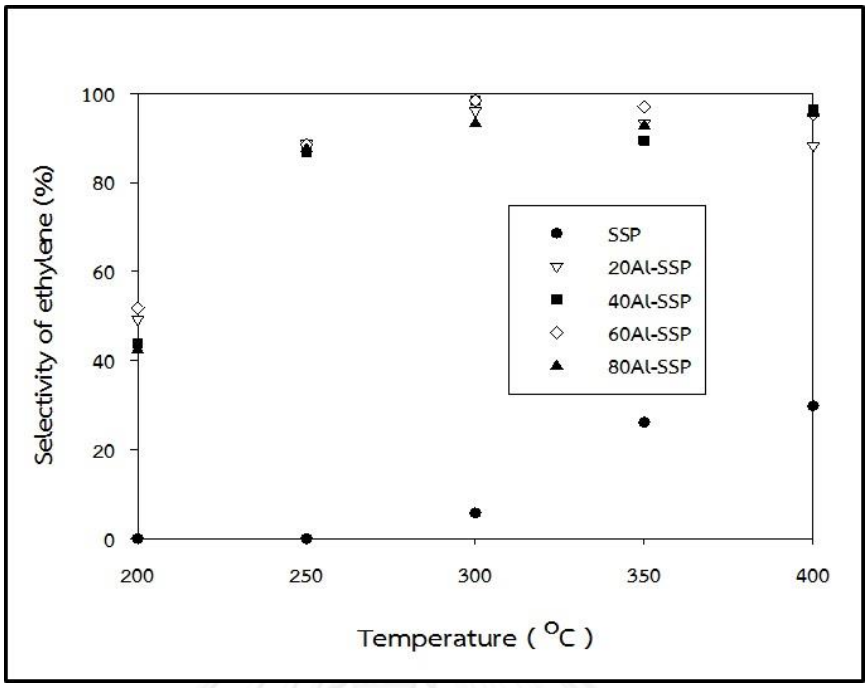

Figure 4. 12 The ethylene selectivity at different temperatures of all catalysts

Figure 4.12 shows the selectivity of ethylene. The results of all catalysts revealed that the selectivity of ethylene is related to the temperature of reaction that it related with ref [10]. The ethylene selectivity of SSP catalyst is the lowest when compared with other catalysts but, it is slightly increased when increasing the temperature. This result agrees with the result of NH_3-TPD, which the acid sites of SSP are the lowest up on the medium-strong acid sites. The ethylene selectivity of all Al-SSP composite catalysts suddenly increased after temperature was increased from 200^{o}C to 250^{o}C. As considering at low temperature, the ethylene selectivity of composite catalysts was resembled. At 200^{o}C and 300^{o}C, the 60Al-SSP provided higher ethylene selectivity than the 20Al-SSP, whereas at the temperature of 250^{o}C, the ethylene selectivity result is opposite with previous temperature result, where the 20Al-SSP exhibited higher ethylene selectivity than the 60Al-SSP. This result can be exhibited for the reason that the 60Al-SSP can donate the highest selectivity of ethylene. It accorded with the result of NH_3-TPD, which the 60Al-SSP exhibited the highest amount of medium-strong acid sites. At high temperature of 350^{o}C-400^{o}C, the selectivity of ethylene was approximately 90 percent. All this results indicated that adding alumina onto silica yielded increased ethylene selectivity.

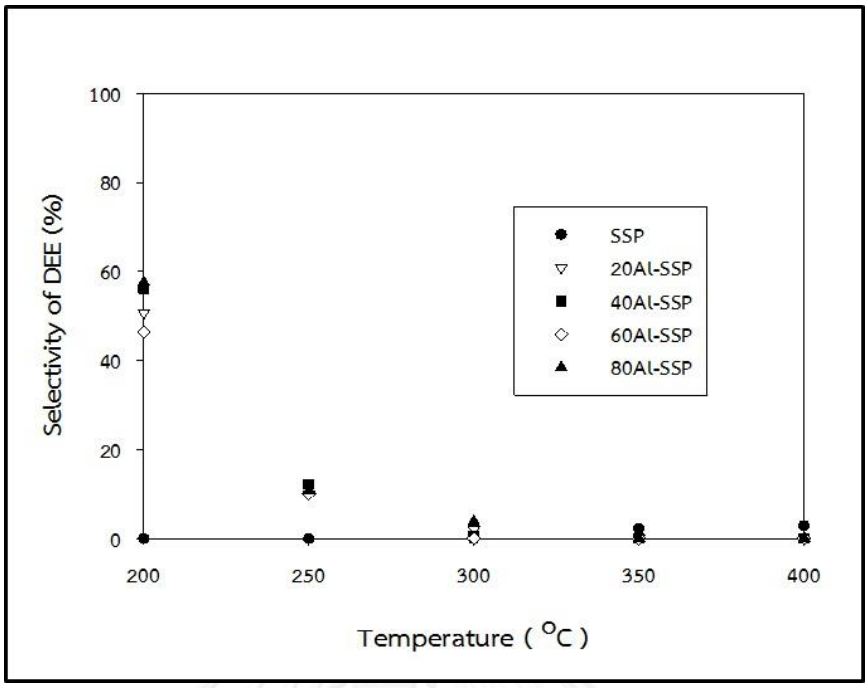

Figure 4. 13 The DEE selectivity at different temperatures of all catalysts

The selectivity of DEE is presented in **Figure 4.13.** The temperature impacted DEE selectivity by which the low temperature gave high DEE. The increase of temperature from 200°C to 250°C can immediately decrease the DEE selectivity. The selectivity of DEE was the highest over the 80Al-SSP that is accordance the amount of weak acid sites present in 80Al-SSP. This result sympathized with [12]. The DEE selectivity was very low on the SSP.

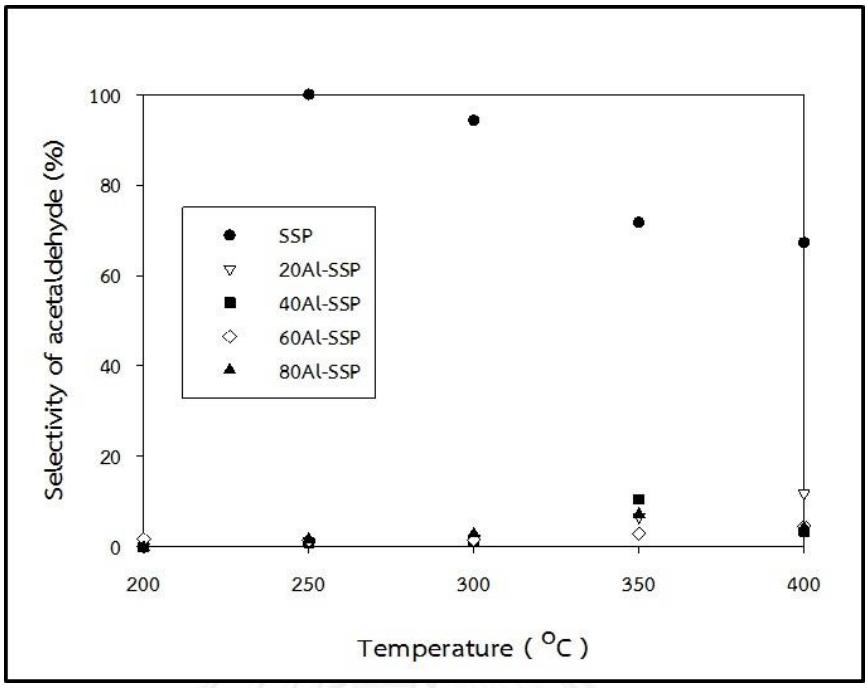

Figure 4. 14 The acetaldehyde selectivity at different temperatures of all catalysts

The acetaldehyde selectivity is displayed in **Figure 4.14.** All composite catalysts gave the acetaldehyde less than pure SSP catalyst. The acetaldehyde selectivity of SSP was suddenly increased from 200°C to 250°C and it was the highest at 250°C, after these it was decreased. This result is accurate with [39] and result of NH_3-TPD which the SSP indicate that exhibited the lowest amount of total acid sites. In addition, the amount of total acid site of all composite catalysts has been closes. So, the selectivity of acetaldehyde was rather uniform.

4.2 Characterization and catalytic activity of 60 weight percent of alumina-silica composite supported molybdenum catalysts.

This section represented the characterization results of 60 weight percent of alumina-silica composite (60Al-SSP) and 60 weight percent of alumina-silica composite (60Al-SSP) supported by various weight percent of molybdenum. The techniques were used in order to investigate characteristic including BET surface area, X-ray diffraction, scanning electron microscopy (SEM), energy dispersive X-ray

spectroscopy (EDX), temperature programmed desorption of ammonia (NH_3-TPD). In the last section, it presented activity of all catalysts in ethanol dehydration reaction.

4.2.1 X-ray diffraction

The X-ray diffraction was used for detection XRD patterns of 60Al-SSP composite catalyst was impregnated by various amounts of molybdenum such as 1wt% 5wt% 12wt% and 16wt% of molybdenum and calcined in air at 550^{o}C for 4 h.

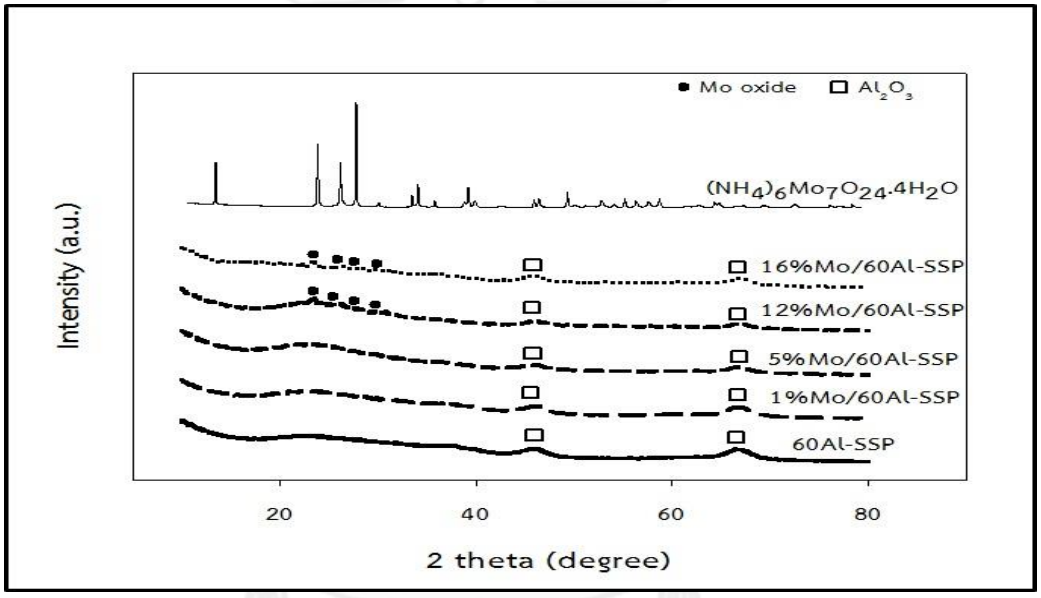

Figure 4. 15 The XRD patterns of all catalysts

The XRD patterns of all catalysts with molybdenum supported on the 60Al-SSP composite catalyst are exhibited in **Figure 4.15**. The XRD peaks of molybdenum oxide forms are presented at 23.2^{o}, 25.5^{o}, 27.4^{o} and 29.6^{o} [7]. The peak of molybdenum oxide was dominated when the modified 60Al-SSP composite catalyst containing more than 12wt% of molybdenum. The peak of γ-Al_2O_3 crystallite remained representing at 45^{o} and 67^{o}. At 1wt% and 5wt% of molybdenum over 60Al-SSP composite catalyst, they did not display the XRD peak of molybdenum oxide form due to the fact that the crystallites size of molybdenum oxide may be less than 3-5 nm or it was well dispersed.

4.2.2 Scanning electron microscopy (SEM)

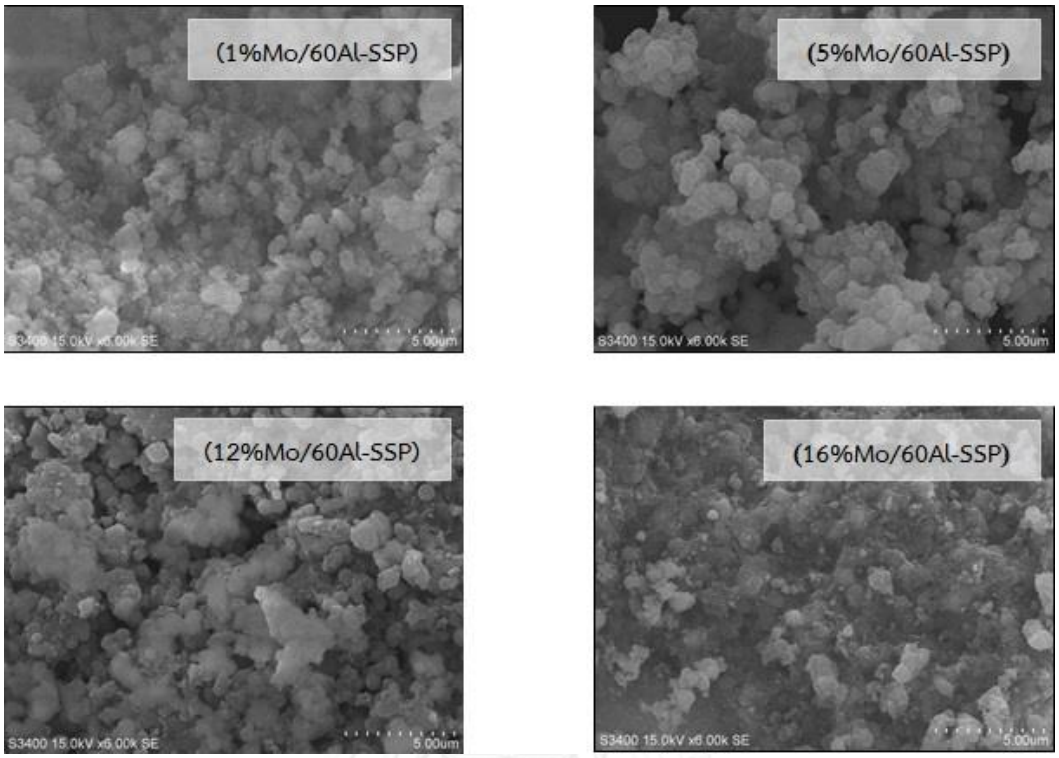

Figure 4. 16 The SEM micrograph of all catalysts

The images of all catalysts, 1wt% 5wt% 12wt% and 16wt% of molybdenum supported 60Al-SSP composite catalyst, are presented in **Figure 4.16**. From these figures, it was found that the morphology of 60Al-SSP composite catalyst did not change after impregnation with molybdenum. The morphologies of all catalysts were similar although there had different amount of molybdenum.

4.2.3 Energy dispersive X-ray spectroscopy (EDX)

Figure 4.17 – Figure 4.20 show the EDX mapping of all catalysts. Alumina, silica, oxygen and molybdenum were distributed on external surface. Those are displayed with white granule. The white granule of molybdenum image was higher when increasing amount of molybdenum. Furthermore, the dispersion of molybdenum was uniform.

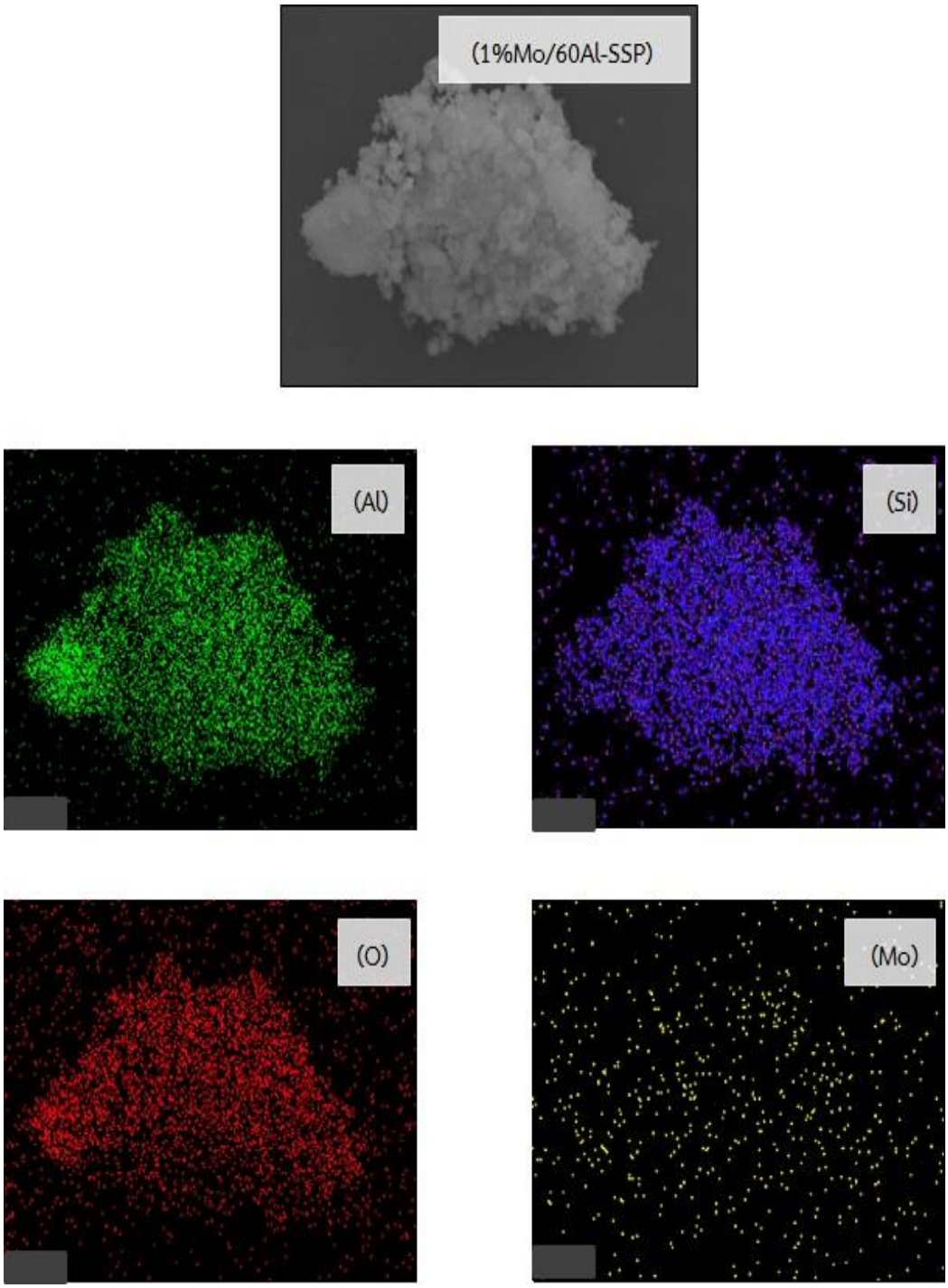

Figure 4. 17 The EDX mapping of 1%Mo/60Al-SSP

.

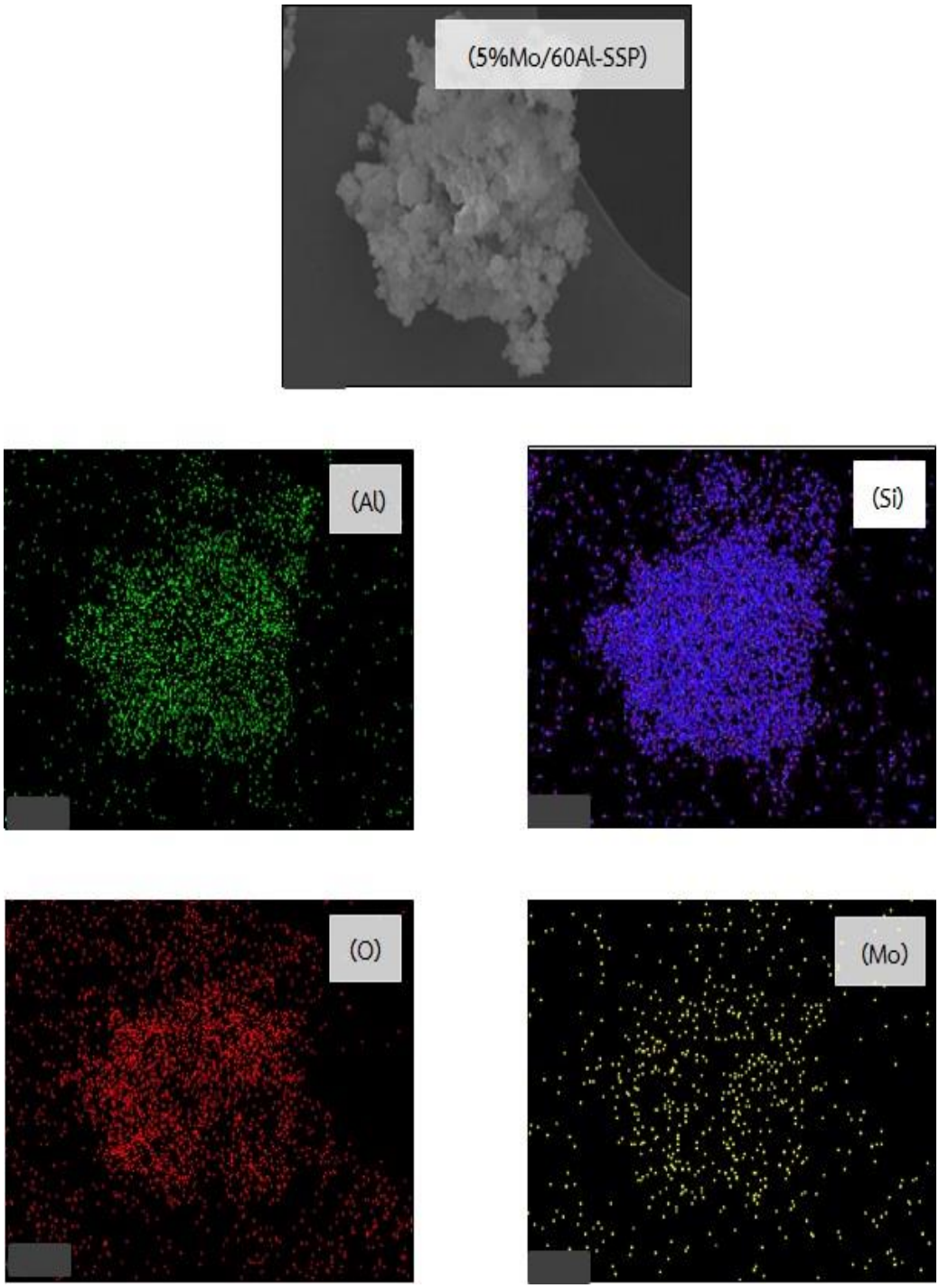

Figure 4. 18 The EDX mapping of 5%Mo/60Al-SSP

.

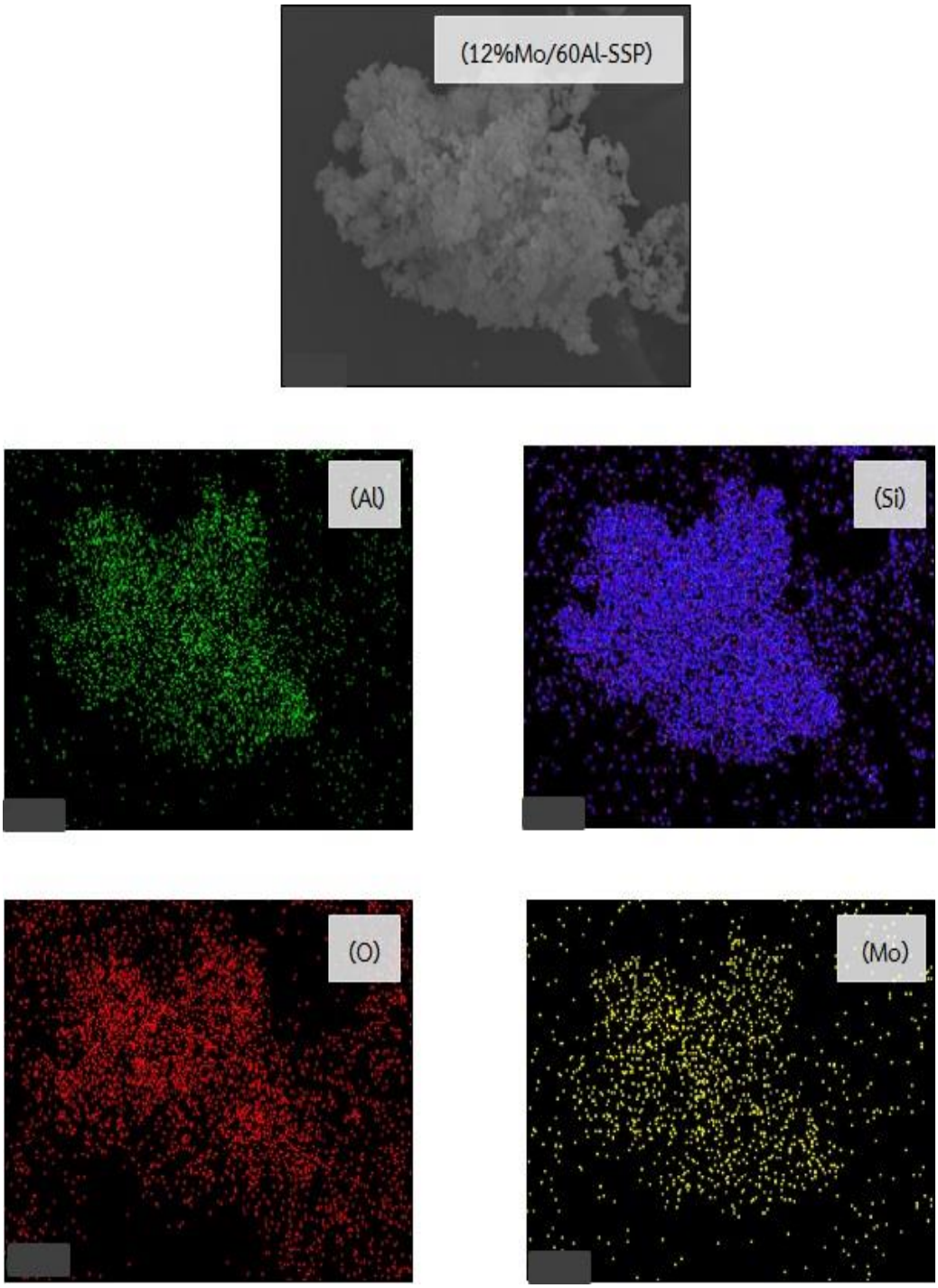

Figure 4. 19 The EDX mapping of 12%Mo/60Al-SSP

.

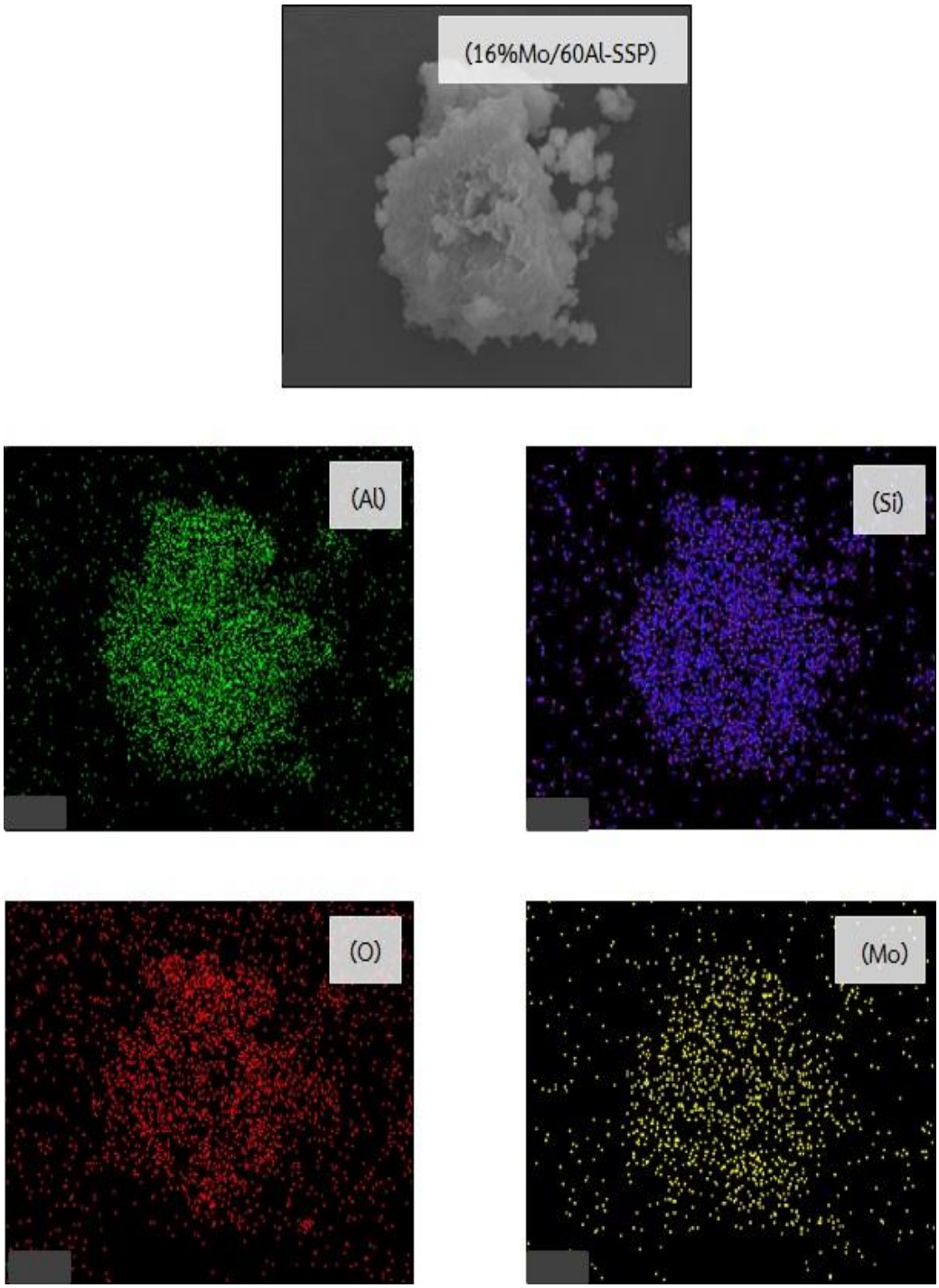

Figure 4. 20 The EDX mapping of 16%Mo/60Al-SSP.

Table 4. 4 The amount of elements distribution on surface of all catalysts.

Catalysts	Amount of weight on surface wt%)			
	Al	Si	O	Mo
60Al-SSP	40.58	7.51	51.90	-
1%Mo/60Al-SSP	27.19	18.54	49.9	4.37
5%Mo/60Al-SSP	13.37	29.31	49.54	7.78
12%Mo/60Al-SSP	11.60	24.88	52.83	10.69
16%Mo/60Al-SSP	23.57	12.21	49.41	14.82

The result of composition on surface of all catalysts was reported in **Table 4.4.** The amount of aluminium in all catalysts decreased when comparing with 60Al-SSP composite catalyst owing to covering by molybdenum. As considering the amount of molybdenum, it was increased by increasing the amount of molybdenum impregnated 60Al-SSP composite catalyst.

4.2.4 Temperature programmed desorption of ammonia

The amount of acid sites of the 60Al-SSP composite catalyst and other molybdenum loaded catalysts are shown in **Table 4.5.** The amount of weak acid sites and medium-strong acid sites depended on the amount of molybdenum loading onto catalysts. The weak acid sites were increased but, the medium-strong acid sites were decreased by higher molybdenum loading. The amount of total acid sites were ranged between 1.70 to 1.99 mmole/g.cat.

Table 4. 5 The amount of acid site of all catalysts.

Catalysts	Number of acid site (mmole/g.cat)		
	Weak	Medium-strong	Total
60Al-SSP	0.25	1.45	1.70
1%Mo/60Al-SSP	0.33	1.37	1.70
5%Mo/60Al-SSP	0.78	1.21	1.99
12%Mo/60Al-SSP	0.97	0.95	1.92
16%Mo/60Al-SSP	1.17	0.79	1.96

4.2.5 Transmission electron microscope (TEM)

The TEM technique was used for investigation of molybdenum particle distribution of all catalysts. This equipment was operated at 200 kV and used magnification at $1x10^6$, $2x10^6$ and $3x10^6$.

The image of distribution at 1wt% and 16wt% of molybdenum particle on 60Al-SSP was shown in **Figure 4.21** and **Figure 4.22**, respectively**.** The black granular in both figures is molybdenum particle distribution. The black granular of 1%Mo/60Al-SSP remained as spherical particle and well distribution. In part of 16%Mo/60Al-SSP, the black granular aggregated and formed to cluster. These results endorsed with ref [7].

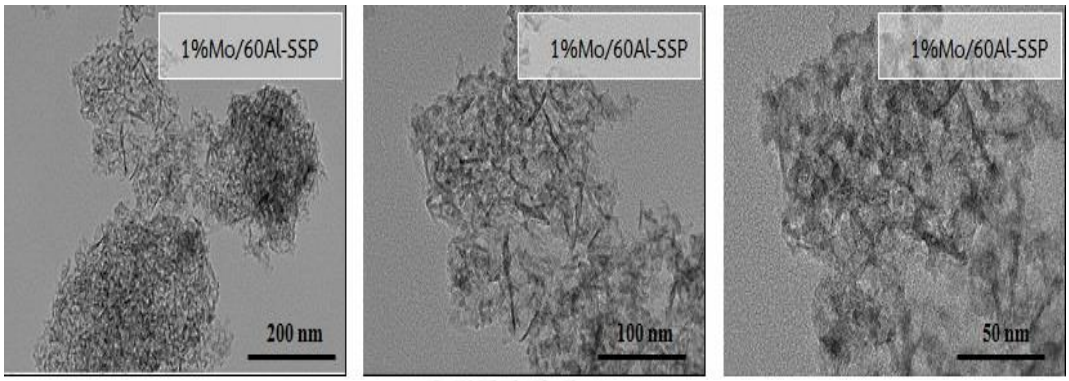

Figure 4. 21 TEM of 1%Mo/60Al-SSP

.

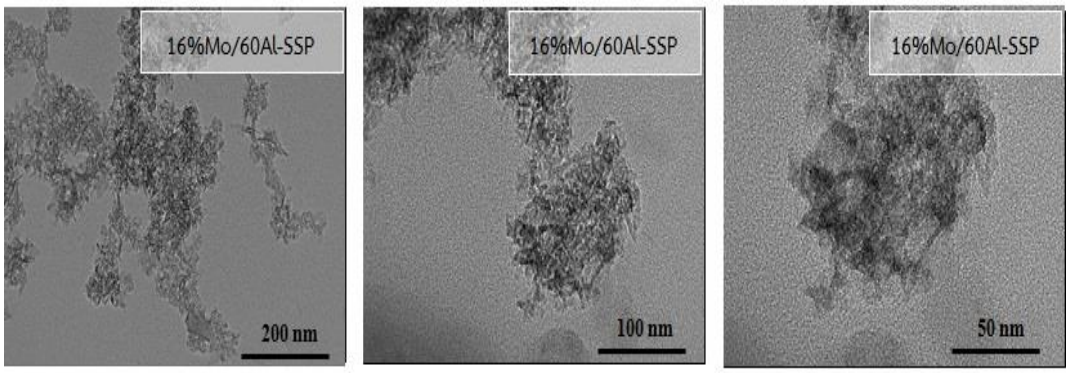

Figure 4. 22 TEM of 16%Mo/60Al-SSP

.

4.2.6 Catalytic activity of 60 weight percent of alumina-silica composite supported molybdenum catalysts in ethanol dehydration reaction.

The performance of 60 weight percent of alumina-silica composite supported molybdenum catalysts was demonstrated by the ethanol conversion and selectivity of products for ethanol dehydration reaction. The catalytic activity results of catalysts are presented in **Figure 4.23** to **Figure 4.26**.

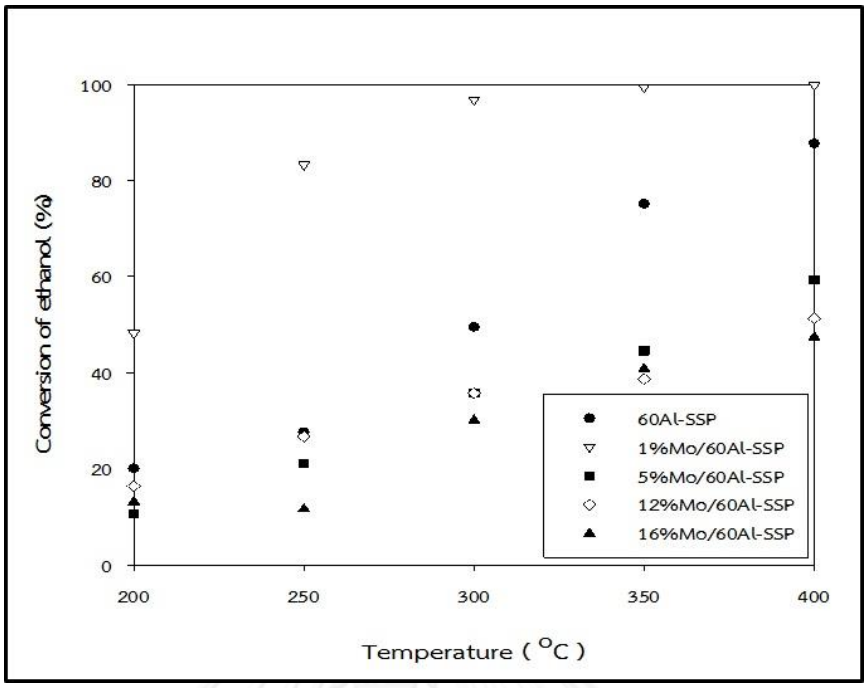

Figure 4. 23 The ethanol conversion at different temperatures of all catalysts

Figure 4.23 shows the ethanol conversion of dehydration reaction. The increased temperature results in increased ethanol conversion of all catalysts and 1%Mo/60Al-SSP exhibited the highest conversion. When comparison between 1%Mo/60Al-SSP and 60Al-SSP, it was found that after loading molybdenum on pure composite catalyst, 1%Mo/60Al-SSP exhibited higher conversion than 60Al-SSP. The other catalysts which contained more than 5wt% of molybdenum exhibited the conversion less than the 60Al-SSP. From this result, it is speculated that the conversion of ethanol depended on rate of reaction. This rate is mention to the ethanol molecules was reacted on both acid site and redox site which was encouraged from adding the molybdenum and this site was used for ethanol dehydrogenation to acetaldehyde [40]. **Table 4.6** exhibited rate of ethylene, acetaldehyde and total rate of all catalysts. The increasing amount of molybdenum on the 60Al-SSP affected the rate of ethylene which was produced on the acid site of catalyst decreased while the rate of acetaldehyde on the redox site of catalyst increased. The total rate includes rate of ethylene and acetaldehyde. The total rate of 1%Mo/60Al-SSP was higher than 60Al-SSP whilst the other catalysts having amount

of molybdenum more than 5wt% gave the total rate lower 60Al-SSP. The total rate agreed with result of ethanol conversion. So, the previous assumption is presumable.

Table 4. 6 The rate of products.

Catalyst	Rate of ethylene*a	Rate of acetaldehyde*b	Total rate*c
60Al-SSP	72.06	-	72.08
1%Mo/60Al-SSP	68.12	5.79	73.91
5%Mo/60Al-SSP	60.13	10.31	70.45
12%Mo/60Al-SSP	47.32	14.17	61.49
16%Mo/60Al-SSP	39.21	19.65	58.86

*Based on 300^{o}C.

*a : Calculated from TOF average of ethylene (s^{-1}) x amount of medium to strong acid site from NH_3-TPD.

*b : Calculated from TOF average of acetaldehyde (s^{-1}) x amount of metal from EDX method.

*c : Total of rate of ethylene and acetaldehyde.

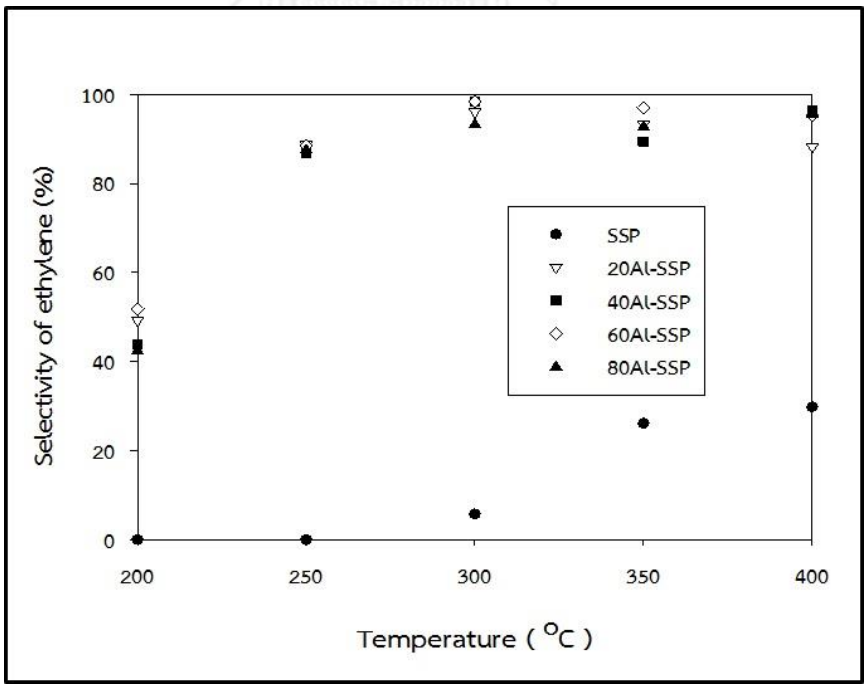

Figure 4. 24 The ethylene selectivity at different temperatures of all catalysts

The ethylene selectivity of ethanol dehydration reaction on molybdenum supported 60Al-SSP composite catalyst is presented in **Figure 4.24.** The increased temperature influenced with ethylene selectivity by increasing the selectivity. The amount of molybdenum in catalysts also affected the selectivity of ethylene. The order of ethylene selectivity is 60Al-SSP > 1%Mo/60Al-SSP > 5%Mo/60Al-SSP > 12%Mo/60Al-SSP > 16%Mo/60Al-SSP. This result conformed with the sequence of number of medium-strong acid sites obtained by NH_3-TPD result. Since, the ethanol dehydration to ethylene required strong acid sites [12], so the prediction that impregnated of molybdenum on 60Al-SSP composite catalyst affected on a decreased of ethylene selectivity.

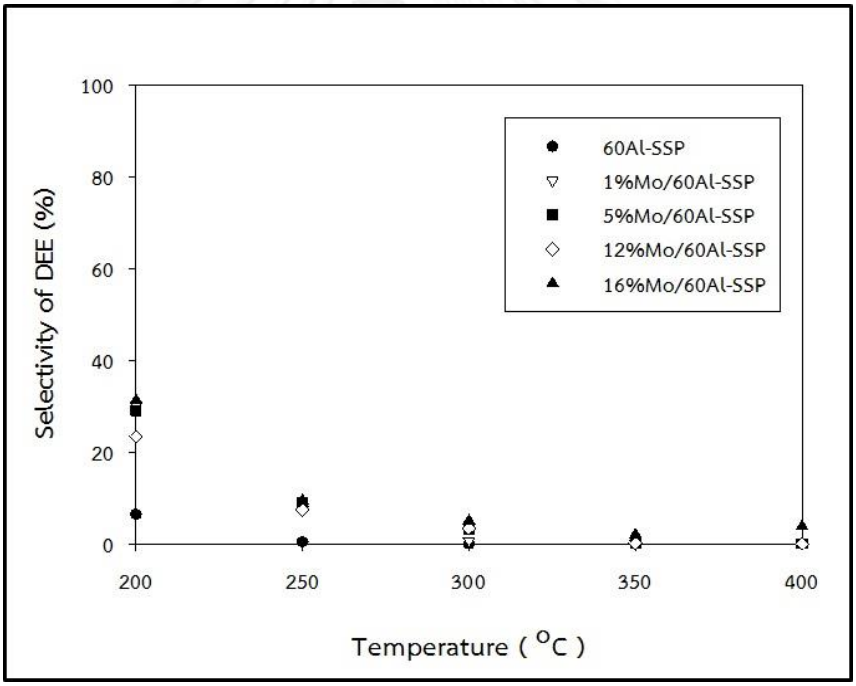

Figure 4. 25 The DEE selectivity at different temperatures of all catalysts

Figure 4.25 represents the selectivity of diethyether (DEE). This result indicated that the DEE selectivity is high at the low temperature. The 16%Mo/60Al-SSP gave the highest selectivity of DEE due to it had the maximum weak acid site based on the NH_3-TPD method. However, the pure composite catalyst, 60Al-SSP, provided poorly selectivity of DEE because this catalyst had the lowest weak acid

sites. So, it was conformable with [12]. Therefore, it was speculated that high loading of molybdenum on 60Al-SSP affected DEE selectivity.

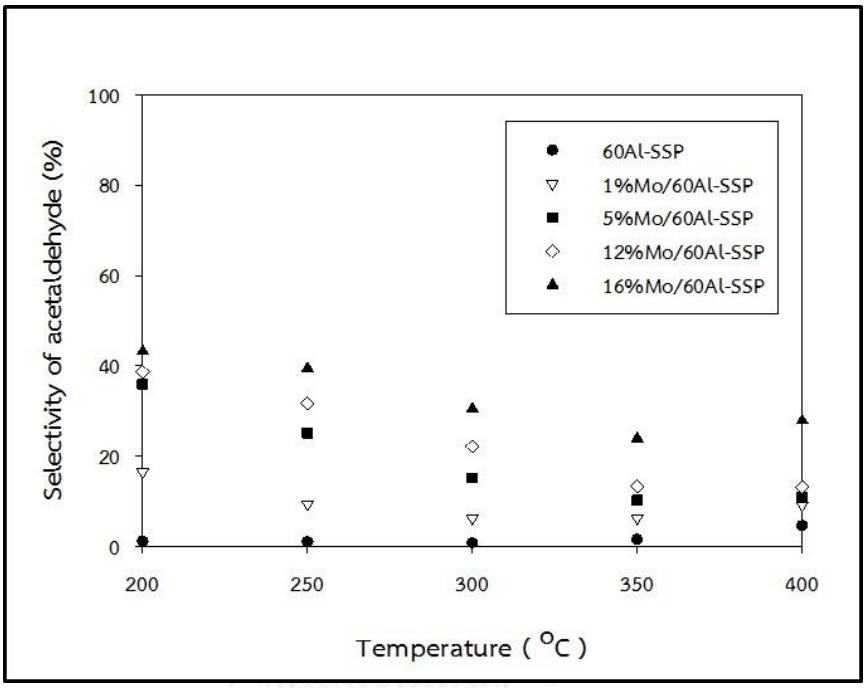

Figure 4. 26 The acetaldehyde selectivity at different temperatures of all catalysts

The loading of molybdenum into 60Al-SSP composite catalyst affected on the selectivity of acetaldehyde as shown in **Figure 4.26**. The 60Al-SSP impregnated with molybdenum gave higher acetaldehyde selectivity when compared with the pure composite catalyst. The increase in temperature resulted in a slight decrease in selectivity of acetaldehyde. The order of acetaldehyde selectivity was 16%Mo/60Al-SSP > 12%Mo/60Al-SSP > 5%Mo/60Al-SSP > 1%Mo/60Al-SSP > 60Al-SSP. This series endorsed with EDX method which represented the concentration of molybdenum on surface of catalyst. So, this resulted may be follow the proposed mechanism of reaction ref. [40].

CHAPTER V

CONCLUSIONS AND RECOMMENDATION

This chapter explained about conclusion of the experimental results which comprised characteristics and catalytic activity of spherical silica particle (SSP), alumina-silica composite (Al-SSP) and 60 weight percent of alumina-silica composite supported molybdenum catalysts for ethanol dehydration reaction. These are described in section 5.1. Moreover, the section 5.2 mentioned recommendation for forward study.

5.1 Conclusions

1. The surface area of SSP and Al-SSP was decreased, whereas average pore diameter was increased by alumina loading. Increasing of alumina did not affect the pore size distribution.

2. The XRD patterns indicated that adding more than 40 weight percent of alumina onto silica, resulted in a larger crystalline size of γ-Al_2O_3.

3. The morphology of SSP and Al-SSP depended on the amount of alumina in the catalysts. The higher alumina led to none spherical particle.

4. The distribution of alumina on silica was uniform and well dispersion.

5. The adding alumina influenced acidity of catalysts. Loading alumina on silica caused the weak acid site and medium-strong acid site increased. The 60Al-SSP exhibited the lowest weak acid sites and the highest medium-strong acid sites.

6. The alumina-silica composite catalysts gave the ethanol conversion, ethylene selectivity and diethylether selectivity higher than those obtained from the spherical silica particle. The acetaldehyde selectivity was the highest on the spherical silica particle.

7. The XRD patterns of molybdenum supported on the 60Al-SSP displayed peak of molybdenum oxide when molybdenum loading was more than 12 weight percent.

8. After impregnated molybdenum on the 60Al-SSP and calcined, the morphologies of catalysts did not change when compared to the 60Al-SSP. Thus, the amount of molybdenum did not feature of catalysts.

9. The concentrations of molybdenum were increased according to the amount of molybdenum loading. There was well distribution.

10. The acid property of catalysts depended on the amount of molybdenum loading. Increasing number of molybdenum decreased medium-strong acid sites, but increased weak acid sites.

11. The 1%Mo/60Al-SSP gave the highest ethanol conversion of dehydration reaction. In part of ethylene selectivity, results followed the amount of medium-strong acid sites, likewise the series of acetaldehyde selectivity, results accorded with concentrations of molybdenum on the 60Al-SSP. All catalysts with molybdenum adding gave the diethlyether selectivity higher than 60Al-SSP pure composite catalyst.

5.2 Recommendations

1. In the further study, the pyridine FT-IR should be used to distinguish types of acid sites included Bronsted acid site and Lewis acid site.

2. The amount of Bronsted acid site are measured by ^{27}Al-NMR technique due to the amount of Bronsted acid site correlates with amount of tetrahedral coordination of Al. Therefore, this technique should be further studied.

3. Other metals should be impregnated onto the alumina-silica composite catalyst shoulder be investigated for development catalytic performancr at low temperature.

4. The other properties of alumina-silica composite catalyst such as thermal stability, life span and coke accumulation etc should be further investigated.

REFERENCES

1. Fan, D., D.-J. Dai, and H.-S. Wu, *Ethylene formation by catalytic dehydration of ethanol with industrial considerations.* Materials, 2012. **6**(1): p. 101-115.
2. Zhang, M. and Y. Yu, *Dehydration of ethanol to ethylene.* Industrial & Engineering Chemistry Research, 2013. **52**(28): p. 9505-9514.
3. Janlamool, J., P. Praserthdam, and B. Jongsomjit, *Ti-Si composite oxide-supported cobalt catalysts for CO2 hydrogenation.* Journal of Natural Gas Chemistry, 2011. **20**(5): p. 558-564.
4. Jetsadanurak., T., *Carbon dioxide Hydrogenation over Alumina-silica composite-supported cobalt catalyst*, in *Chemical Engineering*. 2010, Culalongkorn University.
5. Phongsawat, W., et al., *Role of support nature (γ-Al2O3 and SiO2-Al2O3) on the performances of rhenium oxide catalysts in the metathesis of ethylene and 2-pentene.* Journal of Natural Gas Chemistry, 2012. **21**(2): p. 158-164.
6. Hao, F., et al., *Amorphous SiO2–Al2O3 supported Co3O4 and its catalytic properties in cyclohexane nitrosation to -caprolactam: Influences of preparation conditions.* Journal of Molecular Catalysis A: Chemical, 2012. **363**: p. 41-48.
7. Debecker, D.P., et al., *Flame-made MoO3/SiO2–Al2O3 metathesis catalysts with highly dispersed and highly active molybdate species.* Journal of Catalysis, 2011. **277**(2): p. 154-163.
8. Debecker, D.P., et al., *Opposite effect of Al on the performances of MoO3/SiO2-Al2O3 catalysts in the metathesis and in the partial oxidation of propene.* Applied Catalysis A: General, 2011. **391**(1): p. 78-85.
9. Kitano, T., et al., *Brønsted acid generation of alumina-supported molybdenum oxide calcined at high temperatures: Characterization by acid-catalyzed reactions and spectroscopic methods.* Journal of Molecular Catalysis A: Chemical, 2013. **371**: p. 21-28.
10. Zhang, X., et al., *Comparison of four catalysts in the catalytic dehydration of ethanol to ethylene.* Microporous and Mesoporous Materials, 2008. **116**(1): p. 210-215.
11. Takahara, I., et al., *Dehydration of ethanol into ethylene over solid acid catalysts.* Catalysis Letters, 2005. **105**(3-4): p. 249-252.
12. Madeira, F.F., et al., *Ethanol transformation over HFAU, HBEA and HMFI zeolites presenting similar Brønsted acidity.* Applied Catalysis A: General, 2009. **367**(1): p. 39-46.

13.L.G. Wade, J., *Bimolecular dehydration to form ethers*. Vol. VI. 2006, United State of America Pearson Prentice Hall.
14.*Silica Polymorphs. Available*. 2014; Available from: http://www.crystalmaker.com/library/silica.html.
15.Liu, S., et al., *The influence of the alcohol concentration on the structural ordering of mesoporous silica: cosurfactant versus cosolvent.* The Journal of Physical Chemistry B, 2003. **107**(38): p. 10405-10411.
16.Lebedev, O.I., et al., *Structure and microstructure of nanoscale mesoporous silica spheres.* Solid state sciences, 2004. **6**(5): p. 489-498.
17.Davis, K., *Material Review: Alumina (Al2O3).* School of Doctoral Studies (European Union), 2010: p. 109-114.
18.Santos, P.S., H.S. Santos, and S. Toledo, *Standard transition aluminas. Electron microscopy studies.* Materials Research, 2000. **3**(4): p. 104-114.
19.Shirai, T., et al., *Structural Properties and Surface Characteristics on Aluminum Oxide Powders.* Ceramics Research lab, 2009. **9**: p. 23-31.
20.Santacesaria, E., D. Gelosa, and S. Carrà, *Basic behavior of alumina in the presence of strong acids.* Industrial & Engineering Chemistry Product Research and Development, 1977. **16**(1): p. 45-47.
21.Daniell, W., et al., *Enhanced surface acidity in mixed alumina–silicas: a low-temperature FTIR study.* Applied Catalysis A: General, 2000. **196**(2): p. 247-260.
22.Pieta, I., et al., *Quantitative determination of acid sites on silica–alumina.* Applied Catalysis A: General, 2010. **390**(1): p. 127-134.
23.Leydier, F., et al., *Brønsted acidity of amorphous silica–alumina: The molecular rules of proton transfer.* Journal of Catalysis, 2011. **284**(2): p. 215-229.
24.Poduval, D.G., *On the Role of Acidity in Amorphous Silica-Alumina Based Catalysts.* 2011.
25.Park, J.-I., et al., *Characteristics on HDS over amorphous silica–alumina in single and dual catalytic bed system for gas oil.* Catalysis Today, 2011. **164**(1): p. 100-106.
26.Handzlik, J., et al., *Properties and metathesis activity of molybdena-alumina, molybdena-silica-alumina and molybdena-silica catalysts—a comparative study.* Applied Catalysis A: General, 2006. **312**: p. 213-219.
27.Auroux, A., et al., *Acid sites investigation of simple and mixed oxides by TPD and microcalorimetric techniques.* Thermochimica acta, 2001. **379**(1): p. 227-231.
28.Bentor, Y. *The Periodic Table of the Elements on the Internet*. 1996; Available from: http://www.chemicalelements.com/elements/mo.html.

29.Lifestyle, W. *Molybdenum*. 1996; Available from: http://www.drweil.com/drw/u/ART03381/Molybdenum.html.

30.Liu., Z., et al., *Selective catalytic reduction of NOx by NH3 over MoO3-promote CeO2/TiO2 catalyst.* Catalysis Communications, 2014. **46**: p. 90–93.

31.Winter, M. *Molybdenum crystal structure*. 1993; Available from: http://www.webelements.com/molybdenum/crystal_structure.html.

32.Media, D. *Common Compounds of Molybdenum*. 1999; Available from: http://www.ehow.com/info_8507949_common-compounds-molybdenum.html

33.*Commonly encountered molybdenum compounds*. 1989; Available from: http://www.imoa.info/HSE/environmental_data/chemistry/molybdenum_compounds.php.

34.*Molybdenum compounds in catalysts*. 1989; Available from: http://www.imoa.info/molybdenum_uses/moly_chemistry_uses/moly_compounds/catalysts.php

35.Henker, M., et al., *Structure of MoO,/Al,O,-SiO, catalysts.* Applied catalysis, 1991. **69**(1): p. 205-220.

36.Santos, A.L., et al., *Silica–alumina impregnated with cerium, nickel, and molybdenum oxides for adsorption of sulfur and nitrogen compounds from diesel.* Materials Letters, 2012. **83**: p. 158-160.

37.Debecker, D.P., et al., *Genesis of active and inactive species during the preparation of MoO3/SiO2–Al2O3 metathesis catalysts via wet impregnation.* Catalysis Today, 2011. **169**: p. 60-68.

38.Rajagopal, S., J. Marzari, and R. Miranda, *Silica-alumina-supported Mo oxide catalysts: genesis and demise of Brønsted-Lewis acidity.* Journal of Catalysis, 1995. **151**(1): p. 192-203.

39.SHINOHARA, Y. *A Computational Chemical Investigation of the Dehydration and Dehydrogenation of Ethanol on Oxide Catalysts*. Available from: http://www.sccj.net/CSSJ/jcs/v4n3/a2/text.html.

40.Nair, H., et al., *Mechanistic insights into the formation of acetaldehyde and diethyl ether from ethanol over supported VOx, MoOx, and WOx catalysts.* Journal of Catalysis, 2011. **279**: p. 144-154.

APPENDIX

APPANDIX A

CALCULATION FOR CATALYST PREPARATION

Calculation of Al_2O_3-SiO_2 composite catalysts

The 20% ratios of Al_2O_3 in alumina-silica composite catalyst was prepared by hydrolysis method was shown as follows :

Reagent :
- Alumina isopropoxide 98% ($Al(OPr^1)_3$)
  Molecular weight = 204.25 g/mol
  Alumina (Al_2O_3) formula weight = 101.9614 g/mol
- Support : SiO_2
- Molecular weight of water 18 g/mol
- Ammonia 30%

For 20 %wt. of alumina (Al_2O_3), the support was based on 80 g of silica

The composition of the catalyst would be as follow :

101.9614 g of Al_2O_3 required 408.5 g of $Al(OPr^1)_3$

20 g of Al_2O_3 required $\frac{408.5 \times 20}{101.9614}$ g of $Al(OPr^1)_3$

= 80.13 g of $Al(OPr^1)_3$

$Al(OPr^1)_3$ 98 g provide 98% alumina isopropoxide solution 100 g

$Al(OPr^1)_3$ 80.13 g provide 98% alumina isopropoxide solution $\frac{80.13 \times 100}{98}$ g

= 81.77 g

The ratio of catalyst : isopropanol is 1 : 3 by weight

So, 1 g of catalyst required 3 g of isopropanol

100 g of catalyst required $\frac{100 \times 3}{1}$ g of isopropanol

= 300 g of isopropanol

The ratio of DI water : $Al(OPr^1)_3$ is 4 : 1 by mole

Then, required 80.13 g of $Al(OPr^1)_3$ is changed to mole unit as follow:

204.25 g of $Al(OPr^1)_3$ = 1 mole of $Al(OPr^1)_3$

80.13 g of $Al(OPr^1)_3$ = $\frac{80.13}{204.25}$ mole of $Al(OPr^1)_3$

= 0.39 mole of $Al(OPr^1)_3$

So, required DI water = 4x0.39 = 1.56 mole of water

= 1.56x18 = 28.08 g of water

For ammonia 30%, it included 70% of water

70 g of water in ammonia solution 100 g

28.08 g of water in ammonia solution $\frac{28.08 \times 100}{70}$ g

= 40.11 g

Calculation of molybdenum loading

The incipient wetness impregnation method was used for preparation of molybdenum on the 60 weight percent composite catalyst.

16%Mo/60Al-SSP was prepared as follow:

Reagent : - Ammonium heptamolybdate-tetrahydrat ($(NH_4)_6Mo_7O_{24}.4H_2O$)

Molecular weight = 1,235.86 g/mol

Molybdenum (Mo), atomic weight = 95.94 g/mol

- Support : 60Al-SSP

Based on 1 g of catalyst used, the catalyst composition would be as follow :

Molybdenum	=	0.16	g
60Al-SSP	=	1.00-0.16	g
	=	0.84	g

Mo of Ammonium heptamolybdate-tetrahydrat formula form = 95.96x7

= 671.72 g

671.72 g of Mo in Ammonium heptamolybdate-tetrahydrat 1,235.86 g

0.16 g of Mo in Ammonium heptamolybdate-tetrahydrat $\frac{1,235.86 \times 0.16}{671.72}$ g

= 0.29 g

APPENDIX B

CALIBRATION CURVES

This appendix exhibited calibration curves of reactant and products in ethanol dehydration reaction. There curves were used calculation of composition. The ethanol is reactant while the ethylene is main product but, the diethylether and acetaldehyde are byproducts of this reaction.

The capillary column DB-5 of flame ionization detector (FID), gas chromatography Shimadzu model 14A was used to analyze the concentration of ethanol, ethylene, diethylether and acetaldehyde. The conditions uses in GC are presented in **Table B.1**

Table B. 1 Conditions use in GC-14A.

Parameters	Condition
Width	5
Slope	100
Drift	0
Min.area	300
T.DBL	1000
Stop time	12 min
Atten	2
Speed	3
Method	Normalization
SPL.WT	100
IS.WT	1

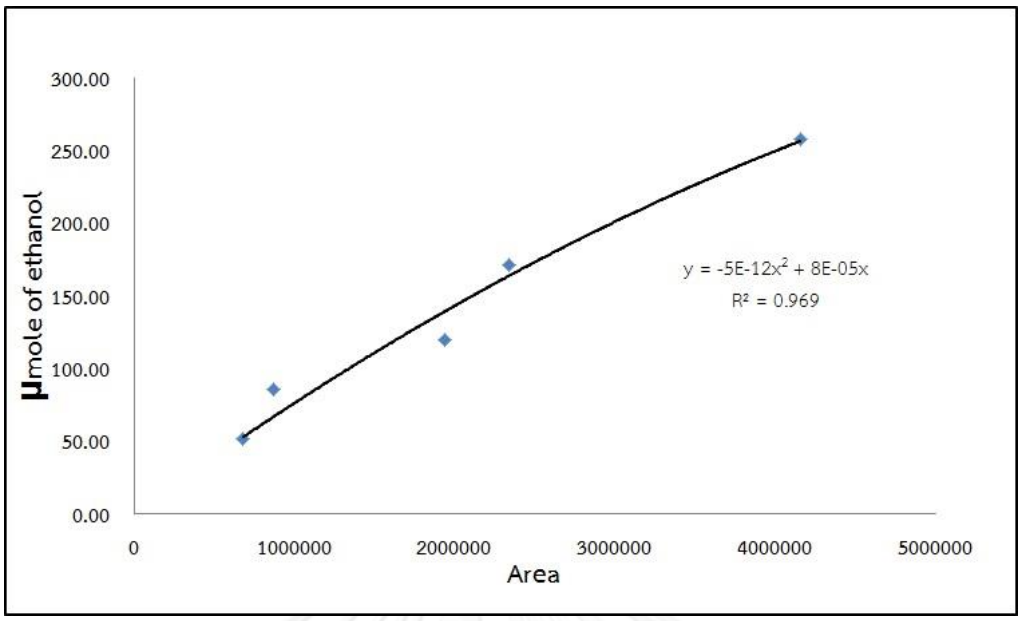

Figure B. 1 The calibration curve of ethanol

.

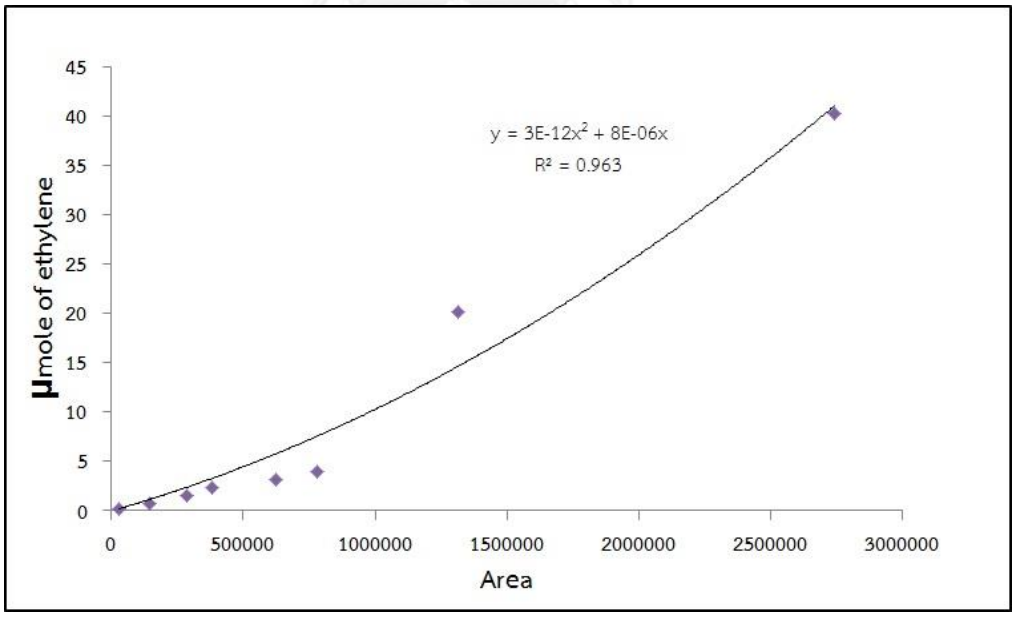

Figure B. 2 The calibration curve of ethylene

.

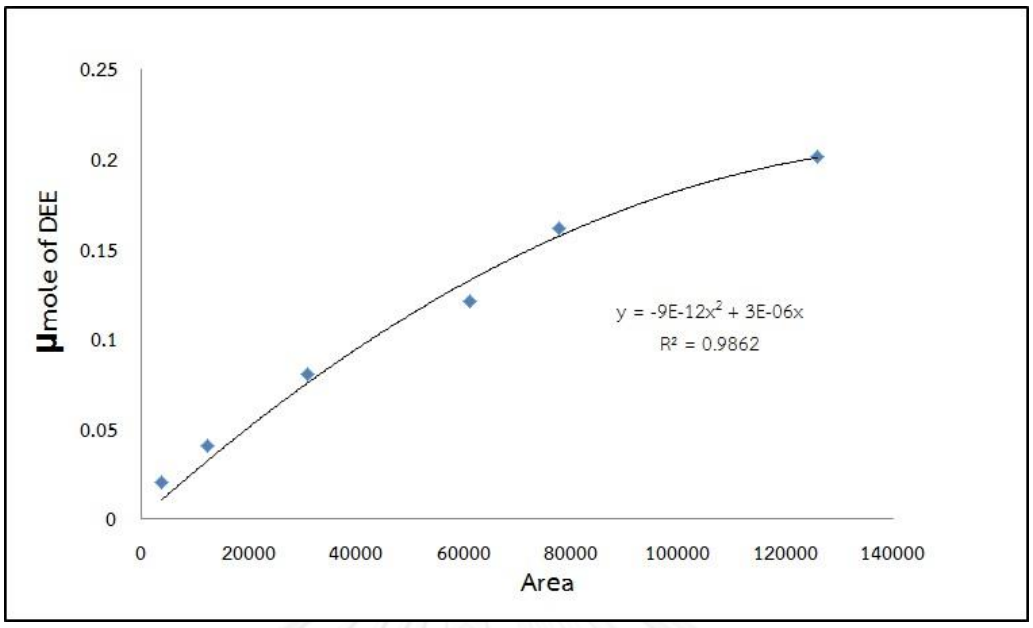

Figure B. 3 The calibration curve of diethylether

.

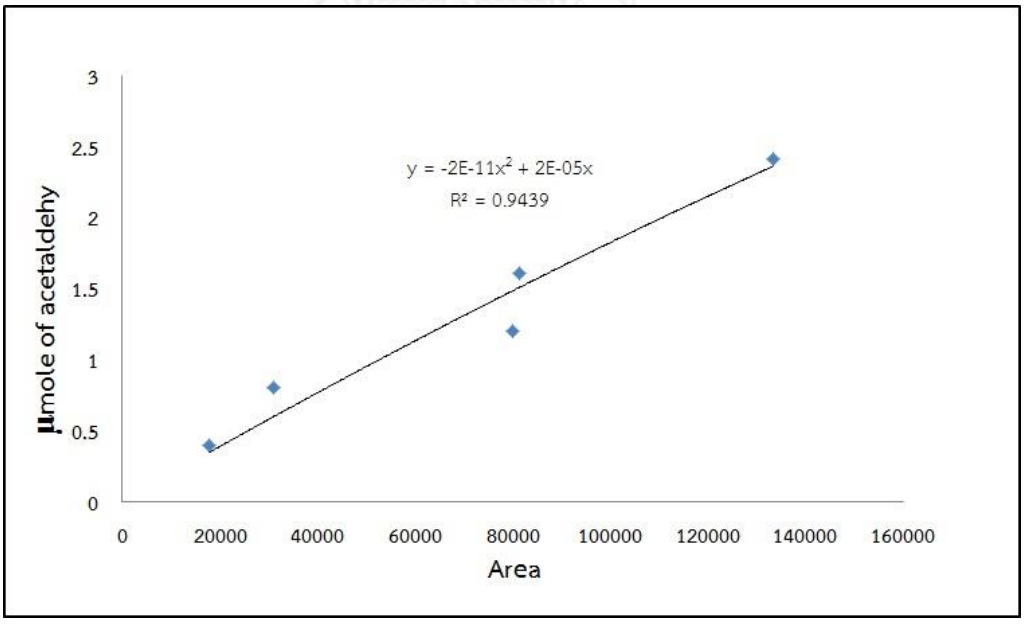

Figure B. 4 The calibration curve of acetaldehyde

.

APPENDIX C

CALCULATION OF ETHANOL CONVERSION AND SELECTIVITY

The conversion of reactant and selectivity of products are performance of catalyst then, there are used demonstrated for ethanol dehydration reaction.

Ethanol conversion

The ethanol conversion is assigned that mole of ethanol converted with respect to ethanol in feed:

$$\text{Ethanol conversion (\%)} = \frac{[\text{mole of ethanol in feed} - \text{mole of ethanol in product}]\times 100}{\text{Mole of ethanol in feed}} \quad \text{(I)}$$

Selectivity of product

The product selectivity is assigned that mole of product (A) formed with respect to mole of ethanol converted:

$$\text{Selectivity of A (\%)} = [\text{mole of A formed} / \text{mole of total products}]\times 100 \quad \text{(II)}$$

Where A is product, the calibration curve of ethylene, diethlyether and acetaldehyde are used measuring the mole of A.

$$\text{Mole of ethylene} = (-2\times10^{-12}) \times \text{area}^2 + (7\times10^{-6}) \times \text{area} \quad \text{(III)}$$

APPENDIX D

CALCULATION OF TURN OVER OF FREQUENCY AND RATE OF REACTION

The changing rate of reaction can be exhibited in term of turn over of frequency or rate of reaction. These can be used explanation transfer rate of reactant molecules to product molecules between reactions.

Rate of reaction

- Reaction rate was based on concentration of A.

$$\text{Rate of A} = \frac{\text{Concentration of A} \times \text{Flow rate of carrier gas} \times 60}{\text{g. of catalyst}} \qquad \text{(IV)}$$

Where The unit of rate of A is μmol/h.g.cat

The unit of concentration of A is μmol/ml.

A is ethylene, diethlyether and acetaldehyde.

Flow rate of carrier gas is 50 ml/min.

g. of catalysts is 0.05 g.

The 60 min/h. in (IV) equation was used for changing the unit of rate of A from μmol/min.g.cat to μmol/h.g.cat.

- Reaction rate was based on amount of active site

Rate of A = Average of TOF of A x Amount of active site (V)

Where The unit of rate of A is μmol/s.g.cat

A is ethylene, diethlyether and acetaldehyde.

TOF is turn over of frequency which it was based on each of temperature ($^{-1}$s).

The amount of active site was based on type of active site for each of product.

Turn over of frequency (TOF)

$$\text{TOF of A} = \frac{\text{Rate of A}}{\text{Amount of active site} \times 3600} \quad \text{(VI)}$$

Where The unit of TOF is $^{-1}$s

The unit of rate of A is μmol/h.g.cat

The unit of amount of active site is μmole/g.cat.

A is ethylene and acetaldehyde.

The amount of active site was based on type of product.

The 3600 s/h. in (VI) equation was used for changing the unit of TOF of A from $^{-1}$h. to $^{-1}$s.

APPENDIX E

CALCULATION OF ACID SITE

The amount of acid site was used representation to acidity of catalyst. The acidity property of catalyst can be measured by various methods. In NH_3-TPD method, the amount of acid site was calculated from area under the curve of TCD signal as a functional of temperature. As following :

$$\text{Amount of acid site} = \frac{Y}{\text{g. of catalyst}} \qquad \text{(VII)}$$

Where The unit of amount of acid site is μmole/g.cat.

g. of catalyst is 0.1 g.

Y is area under the curve x 300 (μmole) which based on calibration curve of micromeritics chemisorp 2750 Pulse Chemisorption System

APPENDIX F

LIST OF PUBLICATION

- **Proceeding**

  Titinan Chanchuey and Bunjerd jongsomjit, “The ethanol dehydration over Al-Si composite catalysts.” Proceeding of the 23rd TIChE National Conference 2013, Khon Kaen University, Thailand, October 17-18, 2013.

The ethanol dehydration over Al-Si composite catalysts

Titinan Chanchuey[1] and Bunjerd jongsomjit

Center of Excellence on Catalysis and Catalytic Reaction Engineering,
Department of Chemical Engineering, Faculty of Engineering,
Chulalongkorn University, Bangkok 10330, Thailand

E-mail: Titinan.Chanchuey@gmail.com

Abstract— In this study, Al-Si composite catalysts were synthesized by adding Al into the spherical silica particle (SSP) having Al loading from 20 to 80 wt%. The dehydration of ethanol on the catalysts was performed in a fix-bed reactor at the atmosphere pressure at various temperatures from 200^{o}C to 400^{o}C. The surface area decreased and the morphology changed with Al addition. The acidity of catalysts depended on Al adding into SSP support. It was found that the 60Al-SSP exhibited the highest ethanol conversion and the ethylene selectivity. Moreover, the temperature range of 300-400^{o}C gave high ethylene selectivity, but the formation of diethylether was found to decrease while the acetaldehyde was low.

Keywords: Al-Si, ethanol dehydration, ethylene

Introduction

In recent years, ethylene is an important light olefin in the chemical industry for production of polyethylene, ethylene dichloride, and ethylene oxide and etc. [1]. For years, ethylene has been produced by the thermal cracking of petroleum gas. When focus on environmental problems, petroleum price and volume petroleum in the world [2], it must find the new source for ethylene production such as methanol or ethanol.

Ethanol is chosen to replace petroleum source because it is clean and renewable [3]. Ethylene was produced by ethanol dehydration reaction over solid acid catalysts such as γ-alumina, zeolite and silica-alumina [4,5]. In the present study, the effect of different Al loading on the spherical silica particle (SSP) on the activity and selectivity during ethanol dehydration to ethylene and other products under the specified operating condition was investigated.

Experimental

A. Catalyst preparation

SSP

First, the spherical silica particle (SSP) was prepared following molar ratio : 1TEOS : 0.3CTAB : 11NH_3 : 58Ethanol : 144H_2O. Secondly, this solution was stirred at room temperature for 2 h after that the white precipitate was separated from solvent by centrifuge. Then, dried sample was calcined in air at 550^{o}C for 6 h [6].

Al-SSP composites

The SSP was added into the solution (desired ratio of aluminum isopropoxide : 2-propanol) and stirred for 1 h at room temperature. Then, adding ammonia [H_2O:Al(OPr^1)$_3$ = 4:1] into the sample for hydrolysis and stirred at room temperature for 20 h. After that the sample was dried at 110^{o}C for 24 h. Dried sample was calcined in air at 650^{o}C for 2 h [6]. The nomenclature of catalysts are XAl-SSP (where X = 20wt%, 40wt%, 60wt% and 80wt%).

B. Catalyst characterization

The surface area, pore volume and pore diameter of catalysts was determined by nitrogen gas adsorption at liquid nitrogen temperature (-196°C) using Micromeritics Chemisorb 2750 Pulse chemisorption system instrument. Before the experiment, the sample was thermally treated at 150°C for 3 h.

The bulk phase of catalyst was determined by SIEMENS D500 X-ray diffractometer (XRD), using CuK_{α} radiation with Ni filter in the 2θ range of 10-90 degrees having the resolution of 0.02^{o}.

The morphology and elemental dispersion over the catalysts surface was determined by Scanning Electron Microscope (SEM) and Energy X-ray Spectroscopy (EDX). The SEM model is JEOL mode JSM-5800LV and Link Isis Series 300 program was performed for EDX.

The acid properties of all catalysts were measured by Temperature Programmed Desorption of Ammonia (NH_3-TPD) equipment by using Micromeritics chemisorb 2750 Pulse Chemisorption System. The catalyst samples were pretreated at 400^{o}C in a flow of helium. The sample was saturated with 15%NH_3/He at 120^{o}C for 1 h. After saturation, the physisorped ammonia was desorped in a helium gas flow. Then the sample was heated from 40 to 800^{o}C at a heating rate 10^{o}C /min. The amount of ammonia in effluent was measured via TCD signal as a function of temperature [7].

C. Catalytic performance

The ethanol dehydration was carried out in a fix-bed down flow reactor at atmospheric pressure and the temperature range of 200-400^{o}C. In this experiment, about 0.05 g of catalyst were packed in reactor. First, a carrier gas (argon) was fed into the reactor for pretreat the catalyst. Ethanol in liquid phase was saturated for 1 h at 200^{o}C, and it was fed into the reactor. The effluent products were collected at 200^{o}C, 250^{o}C, 300^{o}C, 350^{o}C and 400^{o}C. Finally, all samples were analyzed by FID gas chromatograph, using DB5 capillary column.

Results and discussion

D. Catalyst characterization

The trend of catalysts surface area was decreased by adding of Al because Al particle covered on the surface of SSP support. This incidence affects on the morphology of catalysts.

Figure 1 shows the XRD patterns of catalyst. Board peaks around 21-24^{o} represent the conventional amorphous silica [8]. In addition, the maximum sharp peaks center at 45^{o} and 67^{o} can be assigned to the γ-alumina crystallite [8]. The peak of γ-alumina crystallite was dominated when modified SSP catalyst containing more than 40 wt% of Al as shown in Fig.1.

Figure 2 shows the SEM images of catalysts. SiO_2 (a) morphology demonstrated that spherical and smooth surface which was calcined at 550^{o}C. After alumina was loaded into SSP and calcined at 650^{o}C, the morphology of catalysts was displayed in (b), (c), (d) and (e) as 20Al-SSP, 40Al-SSP, 60Al-SSP and 80Al-SSP, respectively. The morphology of catalysts did not remain spherical and being spongy at 80Al-SSP due to coverage by alumina.

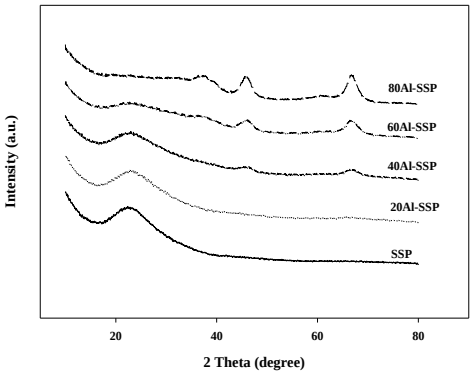

Figure1. XRD patterns of catalysts.

Figure 3 on EDX mapping of catalysts; (b), (c) and (d) images as Al atom, Si atom and O atom, respectively. This image shows only the 60Al-SSP catalyst. The Al atom was thorough dispersion over SSP support. Table 1. shows the amount of Al, Si and O atoms dispersed on the surface of catalysts. The Al atom increased, but Si atom

decreased when adding of Al. Table 2. shows the surface acidity of all catalysts. The assignment of the maximum peak between 175 to 300^{o}C was weak acid site and above 300^{o}C was medium-strong acid site [9]. The total of acid site and medium-strong acid site increased depending on adding of Al. Due to the acidity could be both Bronsted and Lewis acid site, so the total acidity which was increased, maybe comprised Bronsted or Lewis acid site. The s/w ratio was increased by loading Al and its maximum at 60Al-SSP.

E. Catalytic activity

The conversion of ethanol dehydration reaction with temperature range of 200-400^{o}C is shown in Fig.4 indicating that each catalyst exhibited increased ethanol conversion when the temperature was increased. At temperature range of 350-400^{o}C, the ethanol conversion for Al-SSP catalysts went up to 100%, whereas the SSP yielded low conversion. The 60Al-SSP catalyst acted as the best catalyst among other catalysts.

Figure 5 shows the selectivity of ethylene. The SSP catalyst gave the lowest ethylene selectivity at low temperature and slightly increased when increasing the temperature. The ethylene selectivity immediately increased for each catalyst, excepted for SSP when the temperature was increased from 250 to 300^{o}C. All Al-SSP catalysts used in the temperature range of 300-400^{o}C gave about 95% selectivity of ethylene. As consider at 300^{o}C, The 60Al-SSP catalyst gave the highest ethylene selectivity and following 40Al-SSP, 20Al-SSP, 80Al-SSP and SSP, respectively. The ethylene selectivity for 60Al-SSP, 40Al-SSP, 20Al-SSP and SSP agrees with the number of medium-strong acid site, because strong acid site is suitable for ethanol dehydration reaction [10]. The 80Al-SSP exhibited the highest medium-strong acid site, but the ethylene selectivity less than the 60Al-SSP, 40Al-SSP and 20Al-SSP. This was due to the medium-strong acid site of 80Al-SSP may be Lewis acid site, but ethanol dehydration reaction require Bronsted acid site [4]. or medium acid site more strong acid site in total of medium-strong acid site.

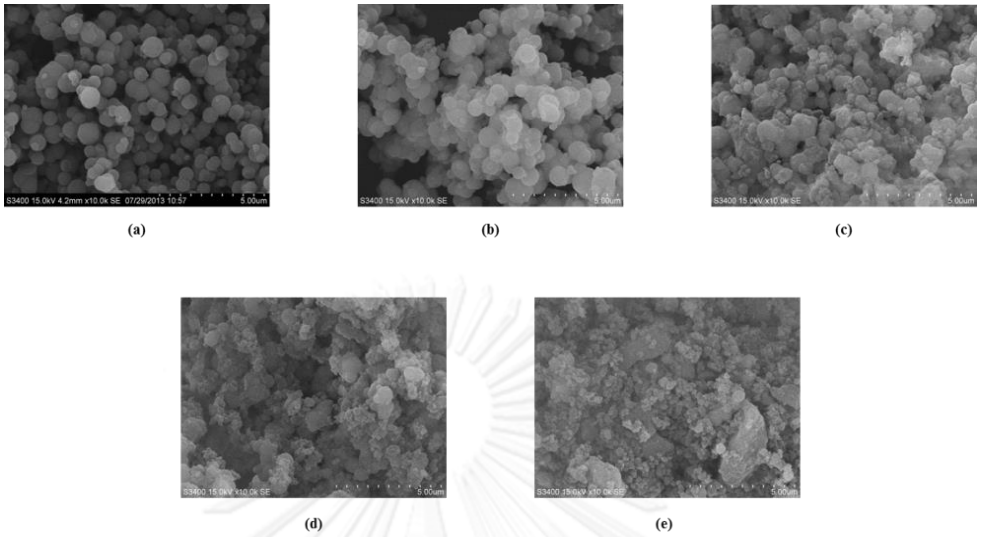

Figure 2. SEM micrograph of all catalyst

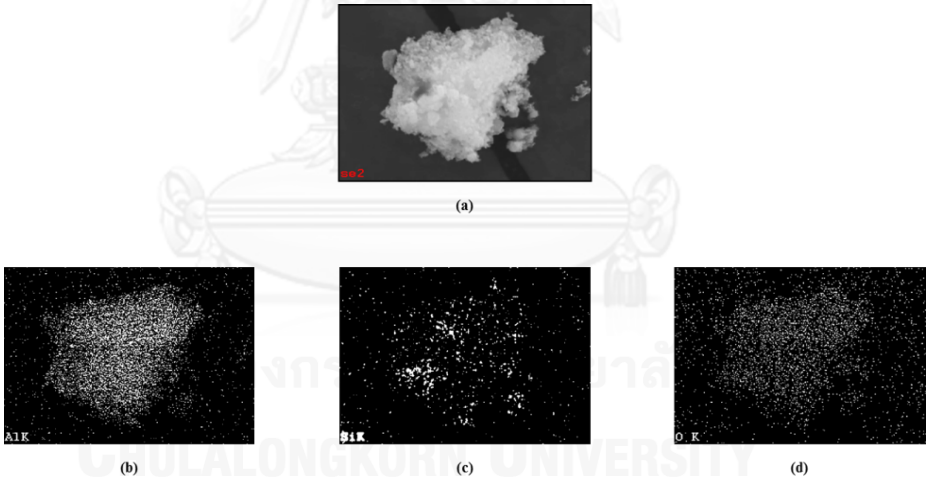

Figure 3. EDX mapping of 60Al-SSP catalys.

Table 1 The amount of atom on surface all catalyst from EDX analysis.

Catalyst	Al (%atom)	Si (%atom)	O (%atom)
SSP	-	31.93	68.07
20Al-SSP	8.69	24.29	67.01
40Al-SSP	21.48	14.41	64.10
60Al-SSP	29.99	5.33	64.68
80Al-SSP	27.78	6.03	66.19

Table 2. The amount of acid site of all catalysts from NH_3-TPD.

Catalyst	Number of acid site (mmole / g. cat.)			S/W ratio
	Weak	Medium-strong	Total	
SSP	0.01	0.00	0.01	0.00
20Al-SSP	0.45	0.00	0.45	0.00
40Al-SSP	0.33	0.31	0.64	0.95
60Al-SSP	0.13	1.27	1.40	10.02
80Al-SSP	0.56	1.75	2.31	3.13

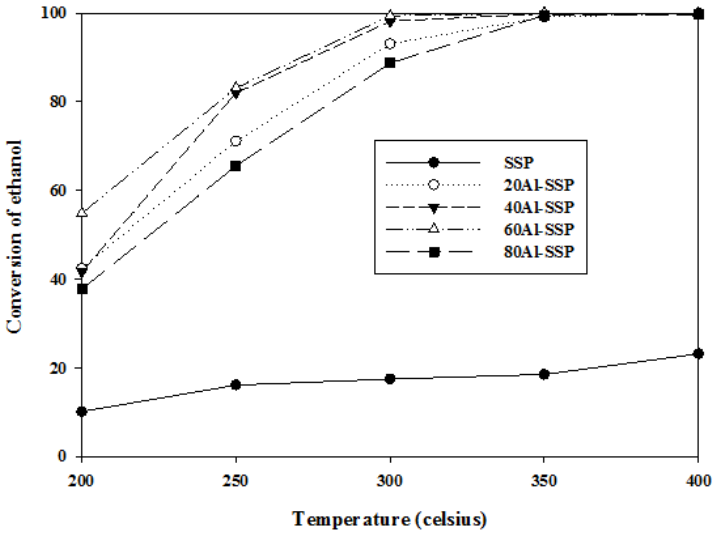

Figure 4. Ethanol conversion at different temperature of all catalysts.

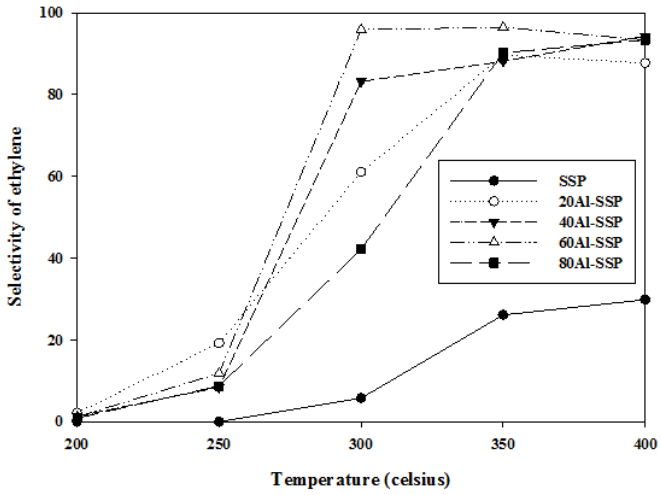

Figure 5. Ethylene selectivity at different temperature of all catalysts.

Figure 6 shows the selectivity of by products on this reaction. The diethylether selectivity was decreased when increasing the temperature, especially the temperature between 250 to 350^{o}C. The diethylether selectivity (DEE) was inversed with ethylene selectivity because the ethanol dehydration to diethylether requires weak acid site [10]. From characterization of NH_3-TPD, it was found that 80Al-SSP exhibited the highest weak acid site. At the low temperature, 200 to 250^{o}C, the acetaldehyde selectivity of SSP catalyst was

immediately increased and slowly decreased when temperature was above 250^{o}C. The other catalysts; 20Al-SSP, 40Al-SSP, 60Al-SSP and 80Al-SSP, gave low acetaldehyde selectivity.

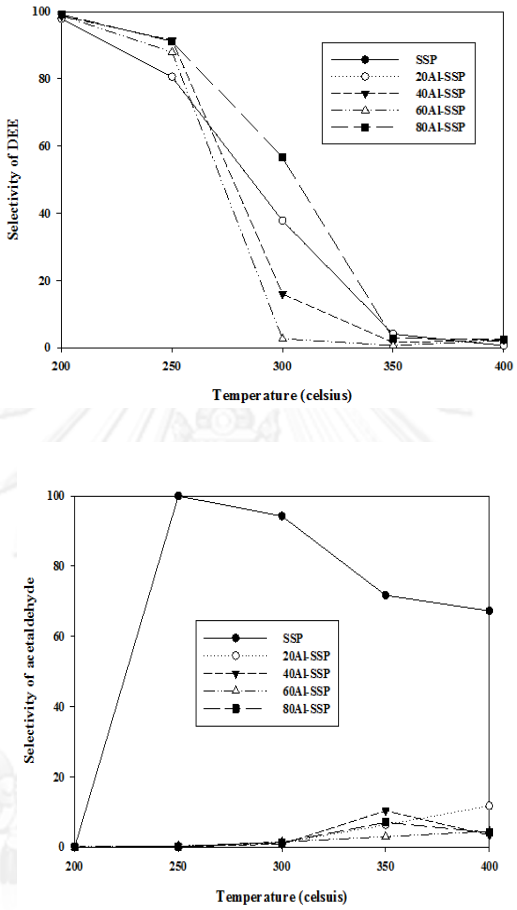

Figure 6. Diethylether selectivity and acetaldehyde selectivity at different temperature of all catalysts.

Conclusions

In summary, the Al-SSP catalysts exhibited high conversion and ethylene selectivity for ethanol dehydration. The 60Al-SSP catalyst performed the highest ethanol conversion. All Al-SSP catalysts gave high ethylene selectivity at high temperature, whereas the other products such as diethylether was high at low temperature. Acetaldehyde selectivity was low based on this study. The ethanol dehydration to ethylene requires strong acid site and Bronsted acid site. The surface area, morphology and acid site of catalysts depend on the amount of Al on SSP support.

References

[1] Xian Zhang, Rijie Wang, Xiaoxia Yang, Fengbao Zhang," Comparison of four catalysts in the catalytic dehydration of ethanol to ethylene", Microporous and Mesoporous Materials 116 (2008) 210–215.

[2] Daisuke Goto, Yasumitsu Harada, Yoshiyasu Furumoto, Atsushi Takahashi, Tadahiro Fujitani, Yasunori Oumi, Masahiro Sadakane, Tsuneji Sano, "Conversion of ethanol to propylene over HZSM-5 type zeolites containing alkaline earth metals", Applied Catalysis A: General 383 (2010) 89–95.

[3] Solange I. Mussatto , Giuliano Dragone, Pedro M.R. Guimarães, João Paulo A. Silva, Lívia M. Carneiro, Inês C. Roberto, António Vicente, Lucília Domingues, José A. Teixeira," Technological trends, global market, and challenges of bio-ethanol production", Biotechnology Advances 28 (2010) 817–830.

[4] Isao Takahara, Masahiro Saito, Megumu Inaba, and Kazuhisa Murata," Dehydration of ethanol into ethylene over solid acid catalysts", Catalysis Letters Vol. 105, Nos. 3–4, December 2005.

[5] J. Bedia, R. Barrionuevo, J. Rodr̊guez-Mirasol, T. Cordero," Ethanol dehydration to ethylene on acid carbon catalysts", Applied Catalysis B: Environmental 103 (2011) 302–310.

[6] Thamonwan Jetsadanurak., Bunjerd Jongsomjit. (2010). Carbon dioxide Hydrogenation over Alumina-silica composite-supported cobalt catalyst.

Master Degree of Engineering Program in Chemical Engineering. Culalongkorn University.

[7] LI Zhong*, MENG Fanhui, REN Jun, ZHENG Huayan, XIE Kechang, Surface Structure and Catalytic Performance of CuCl/SiO2-Al2O3 Catalysts for Methanol Oxidative Carbonylation, Chin J Catal, 2008, 29(7): 643–648.

[8] Weena Phongsawat1, Benjamas Netiworaruksa1, Kongkiat Suriye, Siraprapha Dokjampa, Piyasan Praserthdam1, Joongjai Panpranot1., Role of support nature (γ-Al2O3 and SiO2-Al2O3) on the performances of rhenium oxide catalysts in the metathesis of ethylene and 2-pentene, Journal of Natural Gas Chemistry 21(2012)158–164.

[9] Jarosław Handzlik , Jan Ogonowski , Jerzy Stoch , Maciej Mikołajczyk , and Piotr Michorczyk. Properties and metathesis activity of molybdena-alumina,molybdena-silica-alumina and molybdena-silica catalysts—a comparative study. Applied Catalysis A: General 312 (2006) 213–219.

[10] F. Ferreira Madeira, N.S. Gnep, P. Magnoux, S. Maury, N. Cadran, Ethanol transformation over HFAU, HBEA and HMFI zeolites presenting similar Bronsted acidity, Applied Catalysis A: General 367 (2009) 39-46.

VITA

Miss Titinan Chanchuey was born on June 24th, 1990 in Bangkok province, Thailand. She finished high school from Bodindecha (Sing Singhaseni) 2 in 2007, and received the bachelor's degree of chemical Technology, Faculty of Science, Chulalongkorn University in 2012. She continued her master's study at Department of Chemical Engineering, Faculty of Engineering, Chulalongkorn University in 2014.